NATIONAL TECHNICAL UNIVERSITY OF ATHENS

School of Chemical Engineering

Department of Process Analysis and Plant Design

Thermodynamics and Transport Phenomena Laboratory

Diploma Thesis

By

Verdiana Garofalo

Simulation of Mercury Distribution in Natural Gas Processes

Supervisors:

Epaminondas Voutsas, Associate Professor

Giuseppe Caputo, Associate Professor

Athens, June 2018

Acknowledgements

This Diploma thesis was carried out at the Thermodynamics & Transport Phenomena Laboratory of the School of Chemical Engineering of the National Technical University of Athens.

I would like to thank Associate Professor Epaminondas Voutsas for his availability and his continuous help during my stay at NTUA.

I would also like to thank Associate Professor Giuseppe Caputo for giving me the opportunity to go to NTUA in order to do my Diploma thesis.

I would like to thank Vassilis Koulocheris for his continuous guidance and support during my work in Athens.

In addition, I would like to thank the staff of the laboratory for the support and the advices during my Erasmus period.

I would also like to thank Dr. Efstathios Skouras and Dr. Eleni Panteli from Equinor for the suggestions they provided.

Finally, I am grateful to my family for the support and the encouragement through my studies.

Abstract

Mercury is a trace component that can be found in all fossil fuels and it poses a considerable risk in natural gas processes. The presence of mercury in crude oil and natural gas varies in each stage of extraction, refining and transportation process because it distributes unequally among the vapor, condensate and aqueous phase as a function of pressure and temperature. Mercury causes a wide range of problems in refineries, e.g. equipment degradation, toxic waste generation, serious health impacts and poisoning of catalysts. This is due to its toxicity and its corrosive properties. The amount of mercury in crude oil and natural gas depends on its origins. However, its concentration usually ranges from 1 to 1000 ppb.

Prior to mercury removal, the knowledge of its distribution in the different phases during the separations is necessary. In un-drilled reservoirs the solubility of elemental mercury in the various phases is given by the vapor-liquid-liquid equilibrium. During the drilling process, mercury emerges on the surface with petroleum and is probably redistributed to the various phases due to temperature and pressure changes.

Both the fact that mercury exists at very low concentrations in fossil fuels and can cause major accidents in the natural gas industry, leads to the need of thermodynamic models that can accurately predict the distribution of mercury. The aim of this Diploma thesis is to evaluate two widely used cubic equations of state (EoS) coupled with different expressions for attractive parameter and mixing rules, i.e. SRK-Twu EoS and UMR-PRU EoS-G^E model for simulating a natural gas processing plant and compare the results obtained for mercury partitioning in various streams.

To this purpose, a review of the literature was conducted about mercury, its physical and chemical properties, its species, the most common forms of mercury found in oil & gas, its partitioning in the different compounds and also the reactions in which mercury participates. Afterwards, the SRK-Twu model and the UMR-PRU one, were implemented in the simulation of a real gas processing plant, developed in UniSim and in Aspen HYSYS, in order to compare their tendency to distribute mercury in the different phases during separation. The results showed that mercury is almost equally distributed in the vapor and liquid phase with some differences between the models. In particular, it was seen that UMR-PRU predicts a higher recovery of mercury in the export gas.

Finally, a sensitivity analysis was made by changing the composition of the inlet feed (mercury, water and C7+ concentration) and some operating conditions, i.e. temperature and pressure, in the first three-phase separator. Thus, the new partitioning of mercury between the different phases was checked for both thermodynamic models. In addition, since the fluid under study is a multicomponent system, the distributions of the other components in the outlet streams were also investigated.

KEYWORDS: mercury, natural gas, mercury distribution, thermodynamic model, simulation.

Περίληψη

Ο υδράργυρος είναι συστατικό που εντοπίζεται σε ίχνη σε όλα τα ορυκτά καύσιμα και αποτελεί πηγή κινδύνου για τις διεργασίες επεξεργασίας φυσικού αερίου. Η παρουσία του υδραργύρου στο αργό πετρέλαιο και το φυσικό αέριο ποικίλει σε κάθε στάδιο της εξόρυξης, επεξεργασίας και μεταφοράς, καθώς αυτός κατανέμεται ανισομερώς ανάμεσα στην αέρια, υγρή και υδατική φάση συναρτήσει της πίεσης και της θερμοκρασίας. Ο υδράργυρος προκαλεί πολλά προβλήματα στα διυλιστήρια, π.χ. διάβρωση του εξοπλισμού, παραγωγή τοξικών αποβλήτων, σοβαρές επιπτώσεις στην υγεία και δηλητηρίαση των καταλυτών. Αυτά οφείλονται στην τοξικότητά του και τις διαβρωτικές του ιδιότητες. Η ποσότητα του υδραργύρου στο πετρέλαιο και το φυσικό αέριο εξαρτάται από την προέλευσή τους. Εντούτοις, η συγκέντρωσή του κυμαίνεται ανάμεσα σε 1 και 1000 ppb.

Πριν την απομάκρυνσή του, είναι απαραίτητη η γνώση της κατανομής του στις διάφορες φάσεις κατά τους διαχωρισμούς. Σε ανεκμετάλλευτα κοιτάσματα, η διαλυτότητα του υδραργύρου στις διάφορες φάσεις είναι αυτή που υπαγορεύει η ισορροπία ατμού-υγρού-υγρού. Κατά τη διαδικασία της εξόρυξης, ο υδράργυρος έρχεται στην επιφάνεια μαζί με το πετρέλαιο και πιθανώς ανακατανέμεται στις διάφορες φάσεις λόγω των μεταβολών στην πίεση και τη θερμοκρασία.

Τόσο το ότι ο υδράργυρος βρίσκεται σε πολύ μικρές συγκεντρώσεις στα ορυκτά καύσιμα, όσο και το γεγονός ότι μπορεί να προκαλέσει μεγάλα ατυχήματα στη βιομηχανία του φυσικού αερίου, καθιστούν αναγκαία την ύπαρξη θερμοδυναμικών μοντέλων που να προβλέπουν με ακρίβεια την κατανομή του υδραργύρου. Ο σκοπός της παρούσας Διπλωματικής εργασίας είναι η αξιολόγηση δύο ευρέως χρησιμοποιούμενων κυβικών καταστατικών εξισώσεων (EoS) συζευγμένων με διαφορετικές εκφράσεις για τον ελκτικό παράγοντα και διαφορετικούς κανόνες ανάμειξης, και πιο αναλυτικά των SRK-Twu EoS και UMR-PRU EoS/G^E μοντέλων για την προσομοίωση μιας μονάδας επεξεργασίας φυσικού αερίου και η σύγκριση των αποτελεσμάτων σχετικά με την κατανομή του υδραργύρου στα διάφορα ρεύματα.

Για τον σκοπό αυτόν, έγινε επισκόπηση της βιβλιογραφίας για τον υδράργυρο, τις φυσικές και χημικές ιδιότητές του, τα είδη του, τις πιο κοινές μορφές του στο πετρέλαιο και το φυσικό αέριο, την κατανομή του σε διάφορες ενώσεις και τις χημικές αντιδράσεις

στις οποίες συμμετέχει. Έπειτα, τα μοντέλα SRK-Twu και UMR-PRU χρησιμοποιήθηκαν για την προσομοίωση μιας πραγματικής μονάδας επεξεργασίας φυσικού αερίου με τη βοήθεια των προγραμμάτων UniSim και Aspen HYSYS, ούτως ώστε να συγκριθεί η τάση τους σχετικά με την κατανομή του υδραργύρου στις διάφορες φάσεις κατά τους διαχωρισμούς. Τα αποτελέσματα έδειξαν ότι ο υδράργυρος κατανέμεται σχεδόν ισομερώς ανάμεσα στην αέρια και την υγρή φάση με κάποιες διαφορές ανάμεσα στα μοντέλα. Πιο συγκεκριμένα, παρατηρήθηκε ότι το UMR-PRU προβλέπει μεγαλύτερη ανάκτηση υδραργύρου στο τελικό αέριο προς πώληση.

Τέλος, έγινε ανάλυση ευαισθησίας αλλάζοντας τη σύσταση του ρεύματος εισόδου (υδράργυρος, νερό και κλάσμα C_{7+}) και ορισμένες συνθήκες επεξεργασίας, δηλ. θερμοκρασία και πίεση, στον πρώτο τριφασικό διαχωριστήρα. Έτσι, ελέγχθηκε η νέα κατανομή του υδραργύρου ανάμεσα στις διάφορες φάσεις και με τα δύο θερμοδυναμικά μοντέλα. Επίσης, αφού το υπό μελέτη ρευστό είναι πολυσυστατικό μείγμα, ελέγχθηκε και η κατανομή όλων των υπόλοιπων συστατικών στα ρεύματα εξόδου.

Λέξεις-κλειδιά: υδράργυρος, φυσικό αέριο, κατανομή υδραργύρου, θερμοδυναμικό μοντέλο, προσομοίωση

Table of Contents

List of Tables

List of Figures

Nomenclature

N.G.: natural gas

Hg°: elemental mercury

EoS: Equation of State

SRK-Twu: Soave-Redlich-Kwong Equation of State with Twu's expression for the attractive factor

UMR-PRU: Peng Robinson Equation of State in combination with UNIFAC activity coefficient model by utilizing the Universal Mixing Rules

1. Introduction

Mercury is a toxic chemical element and it is found in all fossil fuels including natural gas, gas condensates, crude oil, coal, tar sands and other bitumens. The concentration of mercury in crude oil and natural gas is highly dependent on geologic location and issues associated with it have become more apparent as deeper and hotter reservoirs are exploited. Mercury enters the global mercury cycle from both natural sources, such as volcanic activity and dissolution of mercury mineral in oceans, and human activities such as industrial activities and combustion of fossil fuel [1].

The U.S. EPA designates mercury and its common chemical forms as persistent, bioaccumulative and toxic pollutants. For this reason, mercury's existence in hydrocarbons raises concerns about equipment degradation, health and safety matters of the field personnel and the environment. Equipment degradation, caused by mercury, is of great importance, especially for the gas industry, because it can lead rapidly to catastrophic failures of the aluminum heat exchangers (Cold Boxes). Specifically, mercury readily forms alloys, called amalgams, with a variety of metals such as aluminum, chromium, copper, zinc, nickel that are weaker than mercury-free metals, causing mechanical failures and gas leaks. One such accident happened in 1973, when a catastrophic failure of an aluminum heat exchanger occurred at Skikda LNG plant in Algeria and led to a plant explosion. Another incident happened in 2004 at the Santos Moomba facility in Australia in the Liquids Recovery Plant (LRP) [2].

Mercury causes significant problems also to catalysts, because it can poison them, it can contaminate product streams and it can lead to gas leaks. Besides, it causes many problems also to the human health [3]. For all these reasons, an investigation on the matter is required. It is, therefore, of great importance for operators to have models that are able to accurately predict mercury's distribution in a processing plant. So, for proper management of mercury in the treatment plants, it is necessary to know the partitioning of the mercury in the different phases during the separations. However, very limited data are available on mercury modelling in the literature, since the models developed by different companies have not been published.

The aim of this Diploma thesis is the implementation of thermodynamic models, which are able to predict the elemental mercury distribution in natural gas, in the simulation of

a typical natural gas processing plant and examine their differences. To this purpose, an overview of the literature is initially undertaken to investigate in depth the properties of mercury and its behavior in natural gas. The two models used are the SRK-Twu and the UMR-PRU models, i.e. two commonly used cubic EoSs, SRK and PR, coupled with different expressions for the attractive parameter and mixing rules. Specifically, they are employed in the simulation of a real gas processing plant in UniSim and Aspen HYSYS and compared in terms of mercury distribution in the various streams. Subsequently, a sensitivity analysis is carried out, by changing the mercury, water and the C_{7+} content in the inlet feed. Besides, some operating conditions, i.e. temperature and pressure, in the plant are also changed in order to examine how the distribution of mercury is modified.

2. Theoretical Background

2.1 Physical and Chemical properties of Mercury

Mercury is the chemical element symbolized as Hg and has the atomic number 80 and molecular weight of 200.59 g/mole. It is a heavy, silver colored, d-block element, and furthermore it is the only liquid metal at standard temperature and pressure (STP) conditions. Its freezing point is -38.83 °C and its boiling point is 356.6 °C. Elemental mercury is quite dense because it has a density of about 13.53 g/cm^3 [4].

The main physical properties of the mercury are summarized in Table 2.1 and they are: its high density and surface tension, its solubility with some metals like gold and silver giving amalgams and its slight solubility in water. On the other hand, mercury is a poor conductor of heat, but it expands and contracts evenly when the temperature changes. It is a fair conductor of electricity [1]. When the temperature is above 40ºC, mercury produces toxic and corrosive vapors heavier than air. Mercury is also harmful by ingestion and inhalation. Moreover, it irritates the skin, the eyes and the breath ways. Another peculiar property of mercury is its high vapor pressure in relation to its atomic weight. The aforementioned characteristics of Hg can be explained by its particular electron configuration, which imparts properties similar to noble gases, such as weak bonds and relative chemical inertia [5].

***Table 2.1** – Properties of Mercury [1]*

Properties of Mercury	
Atomic number	80
Atomic weight	200,59 atomic mass units
Boiling point	356.6 °C
Boiling point/rise in pressure	0.0746 °C/torr
Density	13.53 g/cm^3 at 20 °C
Diffusivity (in air)	0.112 cm^2/sec
Heat capacity	0.0322 cal/g at 20 °C
Henry's law constant	0.0144 atm*m^2/mol
Interfacial tension (Hg/H_2O)	375 dyne/cm at 20 °C
Melting point	-38.83 °C
Saturation vapor pressure	0.16 N/m^3 (pascal) at 20 °C
Surface tension (in air)	436 dyne/cm at 20 °C
Vaporization rate (still air)	0.007 mg/cm^2*hr

Mercury is difficult to oxidize in the natural environment and spilled mercury (in soil for instance) retains the elemental form indefinitely absent moisture and bacteria until evaporation. Mercury is immune to all non-oxidizing acids, but it can be oxidized by the stronger oxidants including halogens, hydrogen peroxide, nitric acid and concentrated sulfuric acid. Mercury is oxidized and methylated in sediments by sulfate-reducing bacteria [1].

Mercury dissolves in concentrated sulfuric acid, nitric acid and aqua regia to give sulfate, nitrate and chloride salts. On the other hand, mercury can react with another metal to form an amalgam. Almost all metals can form amalgams with mercury except iron, copper, manganese and platinum. It is important to emphasize that mercury can corrode aluminum, so it is not advisable to use this kind of metal for the equipment of the oil plant [1].

Mercury occurs mostly in the elemental form or in the inorganic form. Mercury in the atmosphere is mostly elemental, but most of the mercury in water, soil, sediments, plants and animals is in the form of inorganic mercury salts and organometallics [1].

2.2 Mercury in nature

Mercury is a naturally-occurring metal, traces of which are found in rocks of the earth's crust. The most common form in the atmosphere is the uncharged metallic or elemental form (Hg°). Limited amount of elemental mercury may be found in soils and water. In oil and water surface, it is in the mercuric (Hg^{2+}) and in the mercurous (Hg^{+}) states. Inorganic mercury can be methylated by microorganisms native to soils, sediments, fresh water, and salt water, to form organic mercury. Mercury in the environment is constantly cycled and recycled through a biogeochemical cycle, shown in Figure 2.1 [2].

The cycle has six major steps:

1. Degassing of mercury from rock, soils, and surface waters, or emissions from volcanoes and from human activities. This first stage is favored by the surprising degree of volatility of the contaminant.
2. Movement in gaseous form through the atmosphere. Once in the atmosphere, the mercury vapor can circulate for up to a year and become widely dispersed.
3. Deposition of mercury on land and surface waters. mercury is absorbed by surface waters and soil after the elemental mercury vapor suffers a photochemical oxidation to become inorganic mercury that can combine with water vapors and travel back to the Earth's surface as rain.
4. Conversion of the element into insoluble mercury sulfide. This transformation takes place inside the water.
5. Precipitation or bioconversion into more volatile or soluble forms such as methylmercury. The bioconversion is caused by bacteria that process inorganic divalent mercury into methylmercury.

$$Hg^{2+} + bacteria \rightarrow CH_3Hg$$

The reaction depends on the dissolved organic carbon and the pH. Methylmercury is very toxic and accumulates in the body of the living organisms.

6. Reentry into the atmosphere or bioaccumulation in food chains. The methylmercury-processing bacteria may be consumed by the next higher organism up the food chain, or the bacteria may release the methylmercury into the water where it can adsorb to plankton, which can also be consumed by the next higher organism up the food chain.

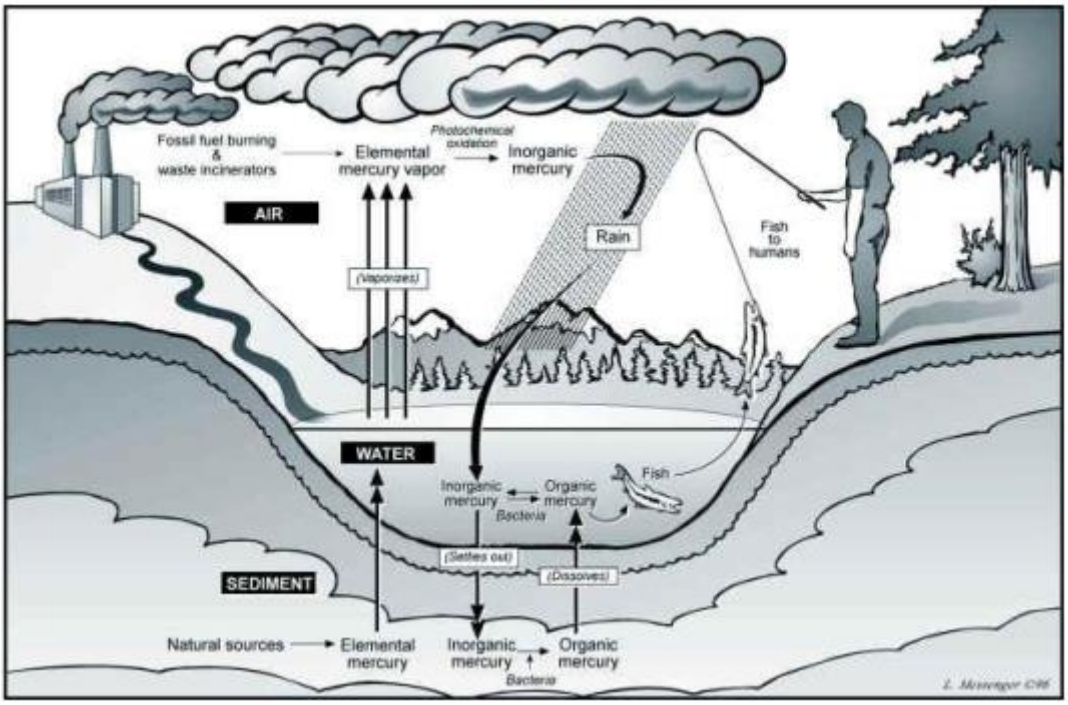

Figure 2.1 *– Biogeochemical cycle of the mercury [2]*

2.3 Mercury in crude oil and natural gas

Crude oil and natural gas are predominantly composed by hydrocarbon atoms, water and a wide spectrum of elements at low levels such as arsenic, vanadium and mercury. So, mercury is a trace component that can be found in all fossil fuels including natural gas, gas condensates, crude oil, coal, tar sands and other bitumens. Thus, production, transportation and processing systems, provide the main opportunity for emissions of mercury to the atmosphere. The mercury associated with petroleum and natural gas

production and processing enters the environment primarily via solid waste streams (drilling and refinery waste) and via combustion of fuels. The amounts in solid wastes and atmospheric emissions from combustion are estimated to be roughly equal [1].

The concentration of mercury in crude oil and natural gas is highly dependent on geologic location and varies between approximately 0.01 ppb and 10 ppm (wt.). Furthermore, mercury deposits are often associated with geological plate boundaries fold belts and areas with volcanic or hydrothermal activity. Issues associated with mercury have become more apparent as deeper and hotter reservoirs are exploited, since higher levels of mercury are found there. The regional estimated levels of mercury in natural gas and condensates are shown in Table 2.2 [1, 6].

Table 2.2 *- Estimated mercury concentrations in natural gas and condensate for world regions [6]*

Location	**Mercury Concentration**	
	Gas (μg/m^3)	Liquids (μg/kg)
Europe	100-150	-
South America	50-120	50-100
Gulf of Thailand	100-400	400-1200
Africa	80-100	500-1000
Gulf of Mexico (USA)	0.02-0.4	-
Overthrust Belt (USA)	5-15	1-5
North Africa	50-80	20-50
Malaysia	1-200	10-100
Indonesia	200-300	10-500

2.4 Mercury risks

Mercury is a considerable risk in natural gas processes. In fact, in most forms, it is toxic and contributes to health, safety and environmental risks. In oil and gas, it has a direct negative impact on petroleum processes. These impacts include equipment degradation, toxic waste generation, increased risk to the health and safety of workers and poisoning of catalysts. Feed of the plants often require process modifications to avoid the negative impacts and to comply with product specifications. Mercury has the ability to form amalgams with other metals (such as Ni, Al, Zn, Au…) and it leads to corrosion of the equipment because the amalgams are frailer than the pure metals. Besides, the amalgams can react with moisture to form metal oxide and free Hg, and the corrosion process is repeated until all metal is oxidized, as in the case of aluminum-based heat exchangers, leading to potential losses to the plant. Because it does not amalgamate with iron, mercury is often stored in containers made of this material [3].

In natural gas treatment plants, a cryogenic distillation process is used to separate ethane and heavy hydrocarbons from sales gas. Furthermore, the components of natural gas liquids (NGL) in the refinery, which are collected by cryogenic distillation, are separated through several thermal fractionation steps based on boiling points. In both treatments, a heat exchanging process is applied, typically using aluminum boxes to facilitate heat exchangers. Unfortunately, Hg can easily degrade the aluminum heat exchangers through three basic mechanisms: amalgamation, amalgam corrosion, liquid metal embrittlement. During amalgamation process, the concentration of Al in the Al-Hg amalgam is relatively low, so defects caused by this mechanism are not in depth. But as mentioned above, aluminum is rapidly oxidized by moisture and thus removed from the amalgam. Al-depleted amalgam therefore dissolves further Al, and this process is repeated until all Al is oxidized [3].

Such mercury-induced corrosion of aluminum heat exchangers resulted in catastrophic failure of heat exchanger at the Skikda LNG plant in Algeria in 1973. Another incident on January 1st 2004 at the Santos Moomba facility in Australia was related to a mercury leak in the Liquids Recovery Plant (LRP). It created a large vapor cloud that ultimately ignited and exploded [2].

As already mentioned, mercury is a risk also for catalysts because it represents the principle cause of their poisoning.

Mercury is a source of risk not only for the health of workers in fossil fuel processing plants, but also for the general population, through its emission to the environment during processing. Its effect on health depends on the chemical form of mercury, its quantity, the person's age and health status, the route of entry to the body (e.g. through breathing, swallowing, skin contact, etc.), the duration of exposure. Particularly toxic are organic mercury compounds, such as methylmercury and dimethylmercury, as well as elemental Hg vapors. Many forms of mercury have the ability of bioaccumulation, whereas the symptoms of contact with some Hg compounds may present after month or years [2].

Short-term exposure to high concentrations of mercury vapor causes harmful effects on the nervous, digestive, respiratory and renal systems. Among the symptoms observed due to high concentration exposures to mercury are fatigue, fever and chills. It is also well known that exposure to any form of mercury can cause damage to the brain, lungs and kidneys or even death, as well as a series of symptoms such as muscle weakness, disorientation, rashes, vision/hearing problems etc. These symptoms also arise in people exposed to 1-44 mg/m^3 of Hg vapor for 4 to 8 hours in a work environment. Deterioration of nerves in the arms and legs has been reported in employees with high exposures [2].

While the symptoms due to long term exposure even to lower concentrations of mercury are mainly related to nervous system damage, manifested as lack of muscle coordination, alteration in behavior, loss of memory, trembling limbs etc. [2].

2.5 Forms of mercury in crude oil and natural gas

Mercury can be found in many crude oil and gas fields. Its presence and concentration depend on many factors, such as: regional-tectonic position, geologic-structural features of the deposit, the operation conditions and seismic activity. However, mercury's concentration varies from about 1 to 1000 ppb, with the mean value close to 5 ppb. As already mentioned Hg^0 has a normal boiling point of 356.62 °C and it would therefore be expected to have a limited distribution in a gas processing plant [1].

In natural gas, mercury occurs in the metallic form. Various forms of mercury, elemental, organometallic and inorganic salt, can be present in natural gas condensates, depending on the origin of the condensates [1].

Mercury can be present in a natural gas mixture and in the condensate phase mainly in the elemental form (Hg^0) due to its volatility, oxidized (Hg^{+1}) and (Hg^{+2}) form, organic or inorganic ionic forms. It can form two kinds of compounds: mercurous, when it uses just one electron in the bonding process (e.g. Hg_2Cl_2) or mercuric, when it uses two electrons to bond with another element (e.g. $HgCl_2$). Mercurous compounds usually involve Hg-Hg bonds and are generally unstable and rare in nature [7].

Mercury occurs in natural gas most prevalently in the elemental form or in the organic mercuric form. Common mercuric compounds include mercuric oxide, mercuric chloride, mercuric sulfide and mercuric hydroxide [7].

Organic compounds contain mercury at the +2-oxidation state. They include organometallic compounds with a Hg-C covalent bond. The two main groups of organic mercury forms are:

- R-Hg-X compounds – partly alkylated species; this group includes mainly monomethyl mercury compounds.
- R-Hg-R compounds – fully alkylated species; this group includes instead dimethyl mercury.

R stands for organic species (e.g. - CH_3), while X for inorganic ions (e.g. chloride, nitrate, hydroxide) [7].

Regarding inorganic compounds of mercury, they include the ionic mercury salts, which can be $Hg^{2+}X$ or $Hg^{2+}X_2$, where X is an inorganic ion. These compounds are soluble in gas condensates, but they prefer to partition to the water phase in primary separations.

Mercury removal is a necessity when natural gas is processed or liquefied in a gas processing or in an LNG plant. In un-drilled reservoirs the solubility of elemental mercury in the various phases is given by the vapor-liquid-liquid equilibrium. During the drilling process, mercury emerges on the surface with petroleum and is probably redistributed to the various phase due to temperature and pressure changes [8].

In order to remove mercury, it is important to determine the various forms of mercury that can be present in oil and natural gas. Various methods have been proposed to categorize mercury. A first distinction is the following [1]:

- Dissolved elemental mercury: it has a solubility in crude oil and in liquid hydrocarbons of a few ppm. It can adsorb on the metal surface and its measured concentration decreases as the distance from the oil or gas well increases.
- Dissolved organic mercury: it is soluble in crude oil and natural gas. Due to difference in boiling point and solubility relative to Hg^0, they are distributed differently in the various distillation fractions.
- Inorganic mercury salts: they are soluble in crude oil and natural gas but are preferably distributed to the aqueous phase during separation. Mercury chlorides are about ten times more soluble in hydrocarbons than elemental mercury.
- Complexed mercury: its existence in produced hydrocarbons is not fully confirmed and depend on the composition of the fluid in question.
- Suspended mercury compounds (HgS): they are insoluble in water and hydrocarbons but can be found in the form of small suspended solid particles.
- Suspended adsorbed mercury: it includes organic and inorganic compounds of Hg that are not dissolved but are adsorbed on inert particles.

There is another classification of the various forms of Hg: dissolved Hg and insoluble Hg. The first can pass through a filter with specific size pore. Insoluble Hg, instead, can't pass through the pore. But this classification doesn't reflect the reality, because if there are particles of Hg that can pass through the filter because they have a size smaller than the pore, they are classified like dissolved but it is not true [8].

In natural gas, mercury is found in its elemental form and in concentration much lower than saturation, indicating the absence of liquid mercury in most reservoirs [9]. Moreover, the cooling of the fluids from the wellhead can cause the condensation of mercury. In gas condensate, the principal form is also elemental mercury but there are also other compounds, such as suspended HgS, dissolved $HgCl_2$, dimethylmercury, CH_3HgCl, etc [1].

Lastly, in high pH amine solutions and glycols, which are extensively used during gas processing, mercury is found predominantly in the form of HgS_2H^- and $Hg(SR)_2$ respectively [8].

It should be noted that the presence of dialkylmercury (RHgR) compounds in produced hydrocarbons is questionable according to a part of the scientific community due to the absence of monoalkylmercury compounds in crude oil samples that would be expected to be similarly abundant with RHgR. The presence of RHgR compounds is usually inferred during analytical measurements when the amount of THg is not equal to the sum of the quantities of individual mercury forms that were determined separately. Although dialkylmercury compounds have been measured directly in some cases, the concentrations were very small and could be attributed to analytical errors [9].

2.6 Partitioning of Hg during natural gas processing

Crude oil contains trace levels of mercury. This contaminant has different impacts in the oil plant processing, in the operators and in the environment. It is for this reason, that in the last years, the distribution of mercury among the gas, oil and water has become an interesting issue for processing engineers. The partitioning of mercury into product and effluent streams in petroleum processing is largely determined by solubility. The approximate solubility of the common mercury species in several liquid matrices is shown in Table 2.3 [1].

Table 2.3 *- Approximate solubility of the common mercury species in several liquid matrices [1]*

Species	Water (ppm)	Oil (ppm)	Glycol (ppm)
Hg^o	0.05	2	<1
XHgX	?	miscible	>1
$HgCl_2$	70,000	>10	>50
HgS	0.01	< 0.01	< 0.01
HgO	50	low	
CH_3HgCl	>10,000	1,000	>1,000

So, for the proper management of mercury in the treatment plants, it is necessary to know the distribution of the mercury in the different phases during the separation. The change in temperature and pressure during migration of fluids to the surface likely re-distributes Hg in the phases. Fluid cooling from the wellhead to surface allows Hg to condense as liquid droplets, which may adsorb onto sand, clays and waxes. A significant part of the total mercury fraction, THg, in gas condensate is comprised of suspended particles in the 1-10 μm range [8].

The distribution of dissolved forms depends on numerous factors including the differences in solubility of each species in the various phases, the chemical composition of the hydrocarbon phases, pressure and kinetic considerations.

Elemental Hg can drop out if the temperature of separator (or pipe) is less than the one of reservoir. Prior to stabilization, both volatile Hg^0 and particulate Hg can be present in the liquid phases. Nevertheless, during stabilization there is a low pressure and, since the vapor fraction increases, more mercury migrates to the vapor phase. This is very effective in stripping dissolved Hg from the crude oil and the condensate. So, additional Hg cannot be stripped from the stabilized fluids. Thus, Hg^0 is predominately found in the stripped gas and in the sediments from inlet separators [1].

Elemental Hg solubility in liquid hydrocarbons increases with increasing number of carbon atoms. Furthermore, solubility is generally higher in straight chain hydrocarbons than branched hydrocarbons or olefins. Moreover, solubility is higher in aromatics than alkanes and increases exponentially with increasing temperature [10].

In polar substances, which are frequently used in natural gas processing, Hg^0 partitioning is expected to follow the general solubility order: alcohols>TEG>MEG>amines>water. In aqueous treating solutions used to dehydrate gas or remove acidic impurities, a portion of Hg^0 can be absorbed in the solution and be desorbed in the regeneration process. This Hg^0 is then present in the regeneration off-gas from these units. So, the presence of common hydrate inhibitors (e.g. MEG, used for natural gas dehydration) increases significantly its concentration in Hg relative to pure water and this is due to the fact that solubility of mercury in alcohols, MEG and TEG is greater than the one in water. In solvents diluted with water, the equilibrium solubility decreases, as expected. Solubility decreases further with increasing water dilution.

Selected solubility and volatility data for elemental mercury and some mercury compounds in water are shown in

Table **2.4** [1].

***Table 2.4** - Solubilities and volatilities of Mercury compounds [1]*

Formula	State	Volatility	Hg Solubility in H_20; 25 C	Name
Hg^0	Liquid	Boiling Point 357 C Vapor Pressure 25 mg/m^3 (25 C)	50 ppb	Elemental
$HgCl_2$	Solid	Boiling Point 302 C	70 g/L	Mercuric chloride
$HgSO_4$	Solid	decomposes 300 C	0.03 g/L	Mercuric sulfate
HgO	Solid	decomposes 500 C	0.05 g/L	Mercuric oxide
HgS	Solid	Sublimes under vacuum; decomposes 560 C	- log $Ksp^{(1)}$ = 52	Mercuric sulfide
HgSe	Solid	Sublimes under vacuum, decomposes 800 C	- log Ksp ~ 100	Mercuric selenide
$(CH_3)_2Hg$	Liquid	Boiling Point 96 C	< 1 ppm	Dimethylmercury
$(C_2H_5)_2Hg$	Liquid	Boiling Point 170 C	< 1 ppm	Diethylmercury

(1) Ksp = solubility product

Inorganic Hg salts are preferably distributed to the aqueous phase during early separation. Suspended mercury compounds, which include HgS but also other mercury species adsorbed on silicates and other suspended colloidal material, are insoluble in oil and water and must be removed with physical methods (e.g. filtration) [8].

2.7 Mercury reactions

Oil and gas processing can cause the transformation of mercury into other forms, but there is very few information about its reactions in open literature. High temperature processes, such as hydrotreating in refineries, should convert dialkylmercury and complexed mercury compounds into elemental mercury. Mercury reacts with elemental

sulfur or sulfuric compounds to form solid metacinnabar (β-HgS). This compound precipitates in tanks and is deposited on equipment walls. The possible reactions are:

$$Hg + S \leftrightarrow \beta\text{-}HgS$$

$$Hg + H_2S \leftrightarrow \beta\text{-}HgS + H_2$$

Both reactions have negative ΔG^0 (-47.7 kJ/mol for the first and -14.3 kJ/mol for the second), so both are spontaneous under ambient conditions [11].

Furthermore, Hg reacts with $HgCl_2$ to form Hg_2Cl_2, a compound that is insoluble in hydrocarbons and precipitates:

$$Hg^0 + HgCl_2 \leftrightarrow Hg_2Cl_2 \downarrow$$

The reaction exhibited a half-life on the order of about 10 days at ambient conditions [12]. However, the origin of $HgCl_2$ in natural gas is not clear. Perhaps, it derives from the reaction of mercury compounds with chloride salts, which are known to be present in reservoir brines.

Also, mercury can be adsorbed on steel pipes with a mechanism of two step reactions [9]:

$$H_2S + Fe_2O_3 \leftrightarrow 2FeO + S + H_2O$$

$$Hg + S \leftrightarrow HgS$$

3. Thermodynamic modelling

In this Diploma thesis an evaluation of the UMR-PRU and SRK-Twu models is made, regarding their ability to predict the partitioning of Hg in a natural gas processing plant.

The critical properties of the mercury employed in this work are shown in Table 3.1. For the other components, the critical properties come from the same source [13].

Table 3.1 *- Critical temperature, critical pressure and acentric factor of Hg [13]*

T_c [K]	1462
P_c [bar]	1608
ω	-0.1645

The main challenge for any model that tries to accurately describe the partitioning of Hg in natural gas systems is the correct prediction of its vapor pressure, which, as already mentioned is abnormally high for its atomic weight. That is why special attention to this issue is given by the employed models, as discussed in the following sections.

3.1 The SRK-Twu Equation of State

The Soave-Redlich-Kwong (SRK) Equation of State is probably the most widely used equation of state in industry for correlating the vapor-liquid equilibria of systems containing non-polar components. The SRK EoS generally gives acceptable vapor pressure predictions at medium and high reduced temperatures for non-polar components but can exhibit large deviations at low temperatures. The calculated vapor pressures tend to diverge from the experimental ones at lower reduced temperatures [14]. The ability of a cubic EoS to correlate phase equilibria of mixtures depends upon the accurate prediction of pure component vapor pressures and mixture properties. Soave suggested that the α function in the Redlich-Kwong EoS should be changed to a different function of temperature in order to improve the prediction of the vapor pressure of pure components and the prediction of multicomponent vapor-liquid equilibria. The temperature-dependent function proposed by Soave, which is a function of the acentric factor, works quite well

for non-polar hydrocarbons. In addition, Soave's function is generally not suitable for polar substances [15].

The SRK-Twu Equation of State is a modification of the classical Soave-Redlich-Kwong EoS. The equation of SRK-Twu model is the same of the original SRK:

$$P = \frac{RT}{(v-b)} - \frac{\alpha(T)}{v(v+b)} \tag{3.1}$$

where

v: molar volume

R: universal gas constant

T, P: temperature and pressure

The difference is in the use of the relationship proposed by Twu et al. [15] for the calculation of the attractive term α, instead of the relationship proposed by Soave. The introduction of this alterative relationship for α leads to a better prediction of the vapor pressure and, consequently, the composition of the gas phase. In fact, Twu's relationship of α is a function of temperature, which takes into account the attractive forces between molecules:

$$\alpha(T) = a(T)\, a_c\,(T_c) \tag{3.2}$$

$$a_c\,(T_c) = 0.427481\ \frac{R^2 T_c^2}{P_c} \tag{3.3}$$

$$a(T) = \ T_r^{N(M-1)} e^{L(1-T_r^{NM})} \tag{3.4}$$

$$T_r = \frac{T}{T_c} \tag{3.5}$$

$$b = 0.086641 \frac{RT_c}{P_c} \tag{3.6}$$

where Tc and Pc are the critical temperature and the critical pressure respectively, T_r is the reduced temperature [15].

The relations in equation (3.4) $a(T) = \ T_r^{N(M-1)} e^{L(1-T_r^{NM})}$ (3.4) contains three parameters, L, M, N, which are unique to each component and they are determined by regressing pure component property data. The L, M, N parameters which

are used for Hg in this Diploma Thesis, have been estimated in a previous Diploma thesis by fitting to experimental data of mercury vapor pressure in the temperature interval of 238.15-1508.15 K [7] and they are shown in Table 3.2. For all other components, the Twu parameters are those employed by Aspen HYSYS.

Table 3.2 *- Twu parameters for Hg [7]*

L	0,09245
M	0,9784
N	2,244

The mixing rules that are being used are the van der Waals One-Fluid [16]:

$$a = \sum_i \sum_j x_i x_j (a_i a_j)^{0.5} \left(1 - k_{ij}\right) \quad (3.7)$$

$$b = \sum_i x_i \, b_i \quad (3.8)$$

where

k_{ij} is binary interaction parameter between component i and component j

x_i, x_j: mole fraction of the component i and component j

The binary interaction parameters of mercury with other compounds, used in this Diploma thesis, have been estimated by Koulocheris et al. [17] and they are presented in **Σφάλμα! Το αρχείο προέλευσης της αναφοράς δεν βρέθηκε.**.

Table 3.3 - *Binary interaction parameters of Hg with various components for SRK-Twu EoS [17]*

Hg° with	**K_{ij}**
CO_2	0.3360
N_2	0.2065
methane	0.0433
ethane	0.0379
propane	0.0624
n-pentane	0.0355
n-hexane	0.0250
n-heptane	0.0042
n-octane	-0.0116
n-decane	-0.0599
n-dodecane	0.0139
i-butane	0.0415
2,2-dimethyl-butane	0.0319
2,2,4-trimethyl-pentane	0.0246
cyclohexane	0.0450
methyl-cyclohexane	0.0266
cis-1,2-dimethyl-cyclohexane	-0.0237
cis-1,4-dimethyl-cyclohexane	-0.0238
trans-1,2-dimethyl-cyclohexane	-0.0094
trans-1,4-dimethyl-cyclohexane	-0.0124
benzene	0.1184
toluene	0.0722
o-xylene	0.0608
water	0.002526*T-0.108422
methanol	0.000918*T+0.174804

Furthermore, for those hydrocarbons that no experimental Hg solubility data are available a generalized correlation was employed. This correlation, estimated by

Koulocheris et al. [17], gives k_{ij} as a function of normal boiling point and molecular weight of hydrocarbon. They are shown in Table 3.4.

Table 3.4 *- Generalized correlation for the k_{ij} between Hg and hydrocarbons for the SRK-Twu EoS [17]*

$K_{ij} = A*T_b + B*MW + C$		
A	**B**	**C**
0.00077	-0.00252	-0.0109

3.2 The UMR-PRU model

UMR-PRU is a predictive model belonging to the category of EoS/G^E models and combines the Peng-Robinson EoS with the UNIFAC activity coefficient model, through the Universal Mixing Rules (UMR). The UMR-PRU model has been developed by the Thermodynamics & Transport Phenomena Laboratory of the School of Chemical Engineering in NTUA. So, this model uses as its basis the Peng-Robinson cubic Equation of State, but instead of the classical mixing rules with the binary interaction parameters (k_{ij}), it introduces the Universal Mixing Rules proposed by Voutsas et al. [18].

The PR model is described by the following equation [19]:

$$P = \frac{RT}{v-b} - \frac{\alpha(T)}{v(v+b)+b(v-b)} \tag{3.9}$$

Where a and b for pure components are calculated by the following equations:

$$\alpha(T) = a(T,\omega)\, a_c\,(T_c) \tag{3.10}$$

$$a_c\,(T_c) = 0.45724\,\frac{R^2 T_c^2}{P_c} \tag{3.11}$$

$$a(T,\omega) = (1 + m(1 - T_r^{0.5}))^2 \tag{3.12}$$

$$m = 0.37464 + 1.54226\omega - 0.26992\omega^2 \tag{3.13}$$

$$T_r = \frac{T}{T_c} \tag{3.14}$$

$$b = 0.07780\frac{RT_c}{P_c} \tag{3.15}$$

Where:

v: molar volume

R: universal gas constant

T, P: temperature and pressure

T_c, P_c: critical temperature and pressure

T_r: reduced temperature

ω: acentric factor

For the satisfactory performance of the model in systems that contain mercury, a modified version of PR has been proposed, which similarly with SRK-Twu utilizes an alternative expression for the attractive term (a) that was proposed by Mathias and Copeman [20], again aiming at improving the prediction of vapor pressure. The relationship proposed by Mathias-Copeman is the following:

$$a = [1 + c_1(1 - T_r^{0.5}) + c_2(1 - T_r^{0.5})^2 + c_3(1 - T_r^{0.5})^3]^2 \qquad (3.16)$$

The terms c_1, c_2, c_3 signify the Mathias-Copeman parameters, which are unique for every component and are calculated by fitting to experimental data of the vapor pressure of the pure components. In a previous Diploma thesis, the Mathias Copeman parameters for mercury were calculated by fitting to experimental vapor pressure data for mercury in the temperature interval 238.15-1508.15 K, as well as the binary interaction parameters for SRK-Twu [7]. They are presented in Table 3.5 – Mathias Copeman parameters for Hg [7].

Table 3.5 *– Mathias Copeman parameters for Hg [7]*

C1	0.14910
C2	-0.16520
C3	0.14470

For the extension to mixtures, the following Universal Mixing Rules (UMR) proposed by Voutsas et al. [18] are applied:

$$\frac{a}{bRT} = \frac{1}{-0.53}\frac{G_{AC}^{E,SG} + G_{AC}^{E,res}}{RT} + \sum_{\mathrm{i}} x_i \frac{a_{\mathrm{i}}}{b_i RT} \qquad (3.17)$$

$$b = \sum_i \sum_j x_i x_j \, b_{ij} \qquad (3.18)$$

$$with \quad b_{ij} = \left(\frac{b_i^{1/2} + b_j^{1/2}}{2}\right)^2 \qquad (3.19)$$

$$\frac{G_{AC}^{E,SG}}{RT} = 5 \sum_i x_i q_i \, ln \frac{\theta_i}{\varphi_i} \qquad (3.20)$$

$$\frac{G_{AC}^{E,res}}{RT} = \sum_i x_i v_k^i \left(ln\Gamma_k - ln\Gamma_k^i\right) \qquad (3.21)$$

$$ln\Gamma_k = Q_k \left[1 - ln\left(\sum_m \theta_m \Psi_{mk}\right) - \sum_m \frac{\theta_m \Psi_{mk}}{\sum_n \theta_n \Psi_{nm}}\right] \qquad (3.22)$$

For component *i*:

$$\varphi_i = \frac{x_i r_i}{\sum_j x_j r_j} \qquad (3.23)$$

$$\theta_i = \frac{x_i q_i}{\sum_j x_j q_j} \qquad (3.24)$$

For UNIFAC group m:

$$\theta_m = \frac{X_m Q_m}{\sum_n X_n Q_n} \qquad (3.25)$$

$$X_m = \frac{\sum_j \nu_m^{(j)} x_j}{\sum_j \sum_n \nu_n^{(j)} x_j} \qquad (3.26)$$

A: parameter equal to -0.53 for PR

r_i: relative van der Waals volume of component i

q_i: relative van der Waals surface area of component i

φ_i: segment fraction of component i

Q_k: relative van der Waals area of sub-group k

x: mole fraction

X_m: mole fraction of group m

$G_{AC}^{E,SG}$, $G_{AC}^{E,res}$: Staverman-Guggenheim terms for the combinatorial and residual parts of the excess Gibbs energy (G^E) respectively

Γ_k: residual activity coefficient of group k in solution

The interaction parameter Ψ_{nm} between groups n and m is a function of temperature, and it is calculated by the following equation:

$$\Psi_{mk} = exp\left[-\frac{A_{nm} + B_{nm}(T - 298.15) + C_{nm}(T - 298.15)^2}{T}\right] \qquad (3.27)$$

where A_{nm}, B_{nm} and C_{nm} are the UNIFAC interaction parameters between groups n and m, which are determined by fitting to binary vapor-liquid equilibrium experimental data [18].

For the extension of the model to systems that contain mercury, Hg is considered as a separate UNIFAC group. The UNIFAC interaction parameters between mercury and other groups have been estimated by Koulocheris et al. [17] by fitting to experimental solubility data and are presented in Table 3.6.

***Table 3.6** – UNIFAC interaction parameters for Hg [17]*

m	n	A_{mn} (K)	B_{mn} (-)	C_{mn} (K^{-1})	A_{nm} (K)	B_{nm} (-)	C_{nm} (K^{-1})
CO_2	Hg	372.86	-2.529	0	160.08	2.718	0
N_2	Hg	320.70	0	0	551.90	0	0
CH_4	Hg	252.30	-2.400	0	505.00	8.270	0
C_2H_6	Hg	392.49	-1.311	0	81.88	1.005	0
CH_2	Hg	290.49	-0.509	0	321.06	1.078	0
bCH_3	Hg	473.50	0.651	0	74.31	-0.415	0
cCH_2	Hg	294.85	-0.145	0	270.08	-0.034	0
ACH	Hg	200.74	-0.643	0	642.39	1.625	0
$ACCH_3$	Hg	535.70	1.909	0	-52.01	-1.410	0
H_2O	Hg	62.30	0.239	0	322.47	-0.888	0
MeOH	Hg	318.26	-0.319	0	276.77	0.851	0

4. Simulation

In this chapter, the two thermodynamic models that were proposed before to predict the behavior of mercury in natural gas were implemented in process simulations. The distribution of mercury in an actual natural gas processing plant was examined, ignoring any reactions in which it participates. To this purpose, only the elemental form of mercury was considered. For the simulations *Aspen HYSYS v8.8* and *Honeywell UniSim Design R451* were used. At the first part, a comparison between the two thermodynamic models was made in order to see how the models tend to distribute mercury among the different phases during separation. The partitioning of mercury in the first three-phase separator and the recovery of mercury in the outlet streams were checked. Furthermore, a k-value analysis was made to better understand the differences between the two models. At the second part, a sensitivity analysis was made changing the composition of the inlet feed and some operating conditions in the flowsheet. Also, in this case, the distribution of mercury in the first three-phase separator and the recovery of mercury in the outlet streams were examined. In addition, the distributions of all components were examined in the outlet streams.

4.1 The natural gas processing plant

The natural gas processing plant under study is a typical plant in Norway. The Process Flow Diagram of the plant is shown in the Figure 4.1.

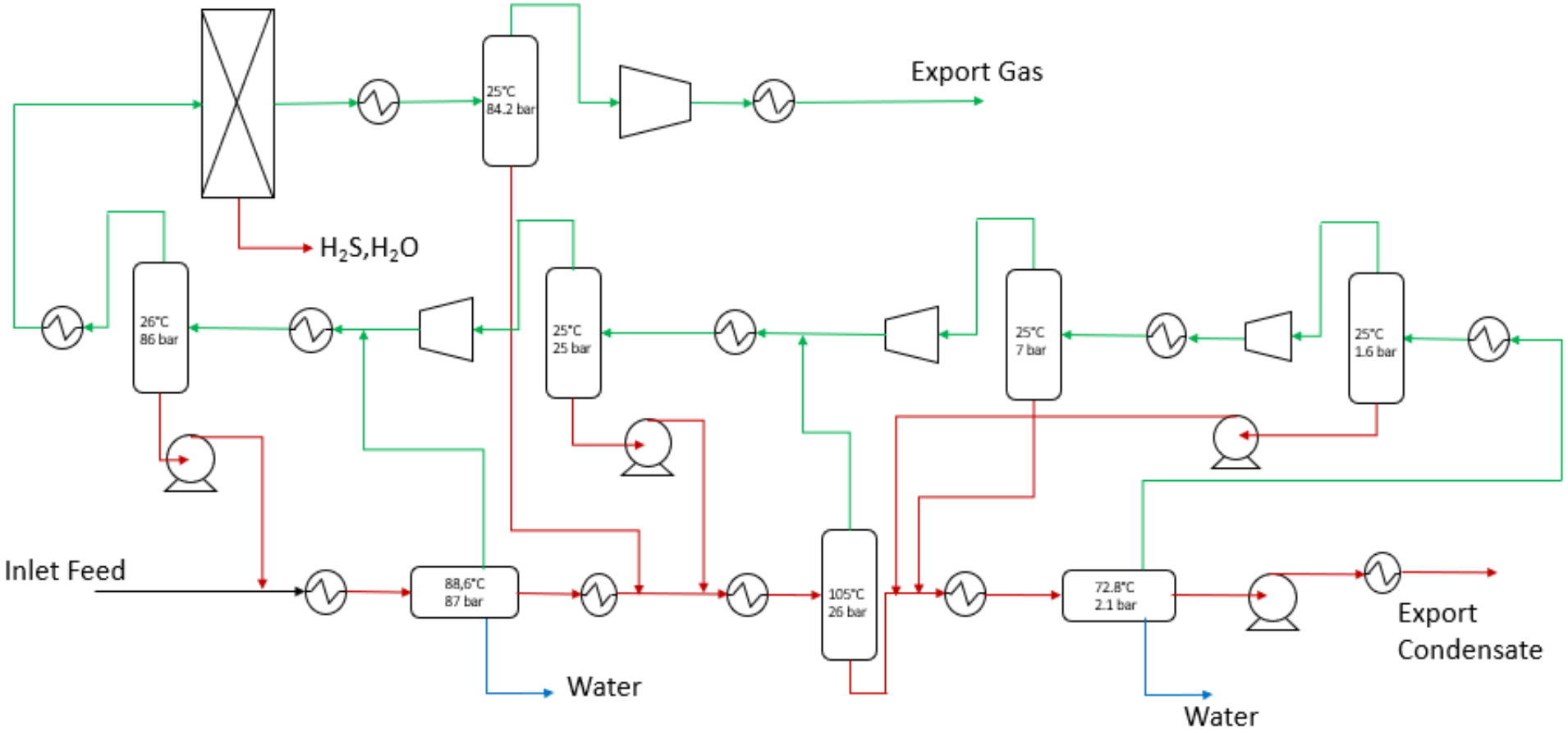

Figure 4.1 - *PFD of the plant under study*

In the plant, there is one inlet feed and four outlet streams, that are the Export Gas, the Export Condensate and the two Water streams. The plant contains two three-phase separators and between them there is a two-phase separator. In these three separators the pressure is gradually decreased to stabilize the stream and to remove the greater amount of water contained in the inlet feed. The vapor products from the two-phase separator and the second three-phase separator pass through three stages of two-phase separators with some in-between compressors to raise the pressure. Then, they are mixed with the vapor product from the first three-phase separator and pass through another two-phase separator operating at a higher pressure. After, they go into a Component Splitter, in order to remove the hydrogen sulfide and the water that are in the gas stream. In reality, this equipment is not present because the sweetening and dehydration processes are included as separate units in the real treatment plant, but for simplicity purposes they were substituted by the splitter. At the end, the gas stream goes into the last two-phase separator in order to remove any traces of heavy hydrocarbons. The final gas is compressed at about 215 bar and cooled until 50 °C for storage or transportation. Finally, the liquid products of the separations return to the stabilizer stage in order to remove the more volatiles components.

A typical molar composition of an inlet feed of a typical natural gas processing plant in Norway is used for the plant under study and it is presented in the Table 4.1. The content of mercury inserted in the composition is 1 ppt, a very low composition.

Table 4.1 *- Typical molar composition of the Inlet Feed*

Component	Composition
H_2O	0.26
N_2	2.3E-03
CO_2	0.03
Methane	0.52
Ethane	0.06
Propane	0.03
i-Butane	6.3E-03
n-Butane	0.01
i-Pentane	4.2E-03
n-Pentane	4.4E-03
GIC6	6.5E03
GIC7	0.01
GIC8	0.01
GIC9	7.7E-03
GIC10-C14	0.02
GIC15-C24	0.01
GIC25+	3.6E-03
H_2S	8.2E-06
Hg	1E-12

It should be noted that Pseudo components are also present in the composition. They are used because it is not known exactly which heavy components are included in the stream. Only the boiling point, the density and the molecular weight are known about Pseudo components and they are shown in Table 4.2.

***Table 4.2** – Properties of Pseudo components*

Pseudo components	Boiling Point [°C]	Density [kg/m^3]	Molecular Weight
GIC6	68.7	665.3	85.5
GIC7	91.9	744.3	91.1
GIC8	116.7	768.3	103.6
GIC9	142.3	785.0	117.2
GIC10-C14	204.0	800.0	155.0
GIC15-C24	317.2	845.7	250.0
GIC25+	480.0	897.7	458.8

4.2 Comparison of SRK-Twu model on HYSYS and UniSim

The process flow diagram of the plant was inserted on Aspen HYSYS for the SRK-Twu model. What concerns the UMR-PRU model, it is not available as a built-in model in commercial process simulators such as Aspen HYSYS, so it was inserted with the help of the CAPE-OPEN platform. This platform gives the opportunity to implement a user-defined model, in this case the UMR-PRU, instead of the thermodynamic models available as built-in in the process simulators. It should be noted that during the simulation through CAPE-OPEN platform on Aspen HYSYS, several convergence problems were encountered. For this reason, it was decided to implement the process flow diagram on UniSim to examine the distribution of mercury with UMR-PRU model. But before this, in order to be sure that Aspen HYSYS and UniSim work in the same way, the results of the simulation with SRK-Twu, with HYSYS, and UniSim were compared. The composition of the inlet feed is set equal to the one presented in Table 4.1. The process flow diagram of the plant inserted on Aspen HYSYS is presented in Figure 4.2 and it is the same with that inserted on UniSim.

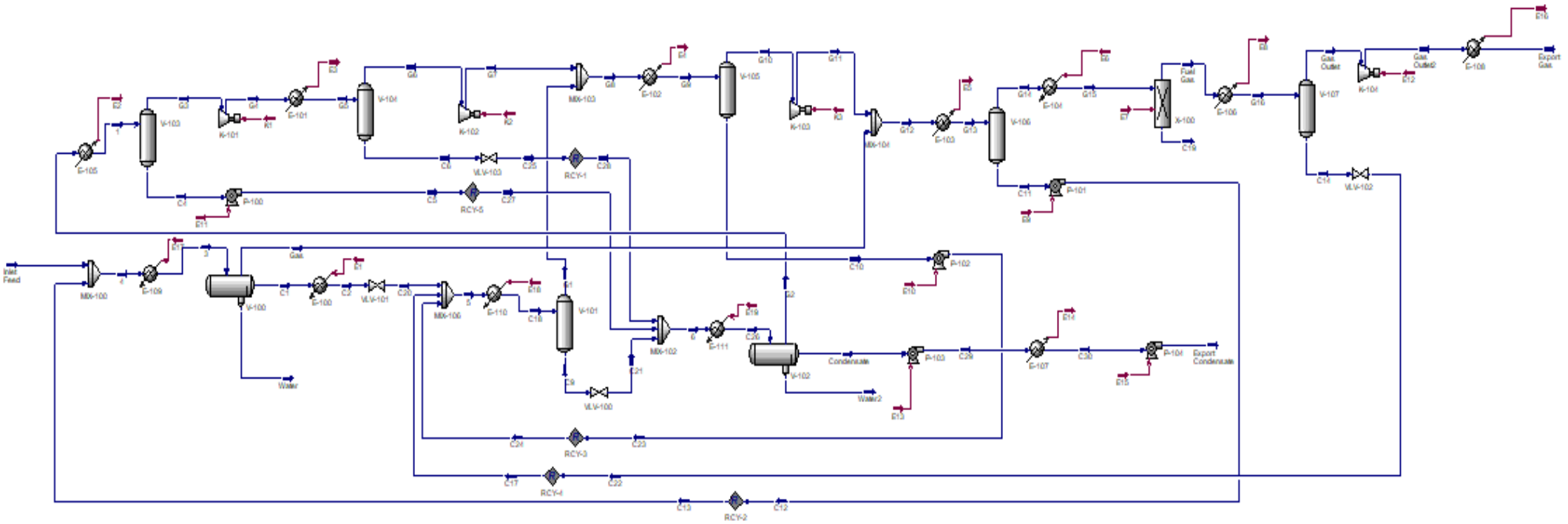

Figure 4.2 – *Process Flow Diagram of the simulation in HYSYS*

The conditions in which the separations take place in the simulation are set equal to those presented in

Figure **4.1** and they are the same for both simulators. During the simulation, the mass balance of Hg was monitored, because it is very difficult to satisfy, and this is due to its very low composition. In the plant, there are five recycle streams, so the program must perform iterations for the calculations of the stream properties (e.g. flowrates, composition etc.), which in the case of Hg have very small values. In order to satisfy the mass balance, the sensitivities of the recycles were reduced up to the point of obtaining a Hg mass deviation lower than 1%. Nevertheless, a production of mercury of 0.22% was observed with SRK-Twu in Aspen HYSYS and a production of mercury of 0.12% with SRK-Twu in UniSim.

The results about the recovery in the first three-phase separator and in the outlet streams were compared, and they are shown in

Table **4.3** and

Table **4.4** respectively. It should be noted that recoveries are calculated with respect to the inlet feed.

In addition, the K-values were examined. Below, the K-value expression for the organic and aqueous phases can be found along with the results of the analysis. The K-values for the first three-phase separator are shown in Table 4.5.

$$K = \frac{y}{x_{org}} \tag{5.1}$$

$$K = \frac{y}{x_{aq}} \tag{5.2}$$

Where

y: mercury composition in vapor phase

x_{org}: mercury composition in organic phase

x_{aq}: mercury composition in aqueous phase

Table 4.3 - *Hg Recovery in the first three-phase separator of the simulation with SRK-Twu on HYSYS and UniSim*

	Hg Recovery		
	Liquid Phase	**Vapor Phase**	**Water Phase**
Aspen HYSYS	40,5%	59,3%	0,23%
UniSim	40,4%	59,4%	0,23%

Table 4.4 – *Hg recovery in the Outlet Streams of the simulation with SRK-Twu on HYSYS and UniSim*

	Hg Recovery	
Outlet Stream	**Aspen HYSYS**	**UniSim**
Export Gas	47,24%	47,15%
Export Condensate	52,72%	52,71%
Water	0,26%	0,26%

Table 4.5 – *K values for Organic and Aqueous Phases in the first three-phase separator of the simulation with SRK-Twu on HYSYS and UniSim*

	K_{org}	**K_{aq}**
Aspen HYSYS	0,13	67,5
UniSim	0,13	67,9

Comparing the results of the simulation with the SRK-Twu model, implemented in Aspen HYSYS and in UniSim, the first observation is that identical results were obtained. This means that, for the case under study, the two simulators work in the same way.

4.3 Comparison between SRK-Twu model and UMR-PRU model

The simulations were carried out with the two thermodynamic models already mentioned in the previous chapter. The distribution of mercury in the natural gas processing plant was examined ignoring any reactions in which Hg participates. The operating conditions of each separator in the simulation are set equal to those presented in

Figure **4.1** for both thermodynamic models. Also, in this case, the sensitivities of the recycles present in the plant were reduced in order to satisfy the mercury mass balance. A production of mercury of 0.12% was observed with SRK-Twu and a loss of mercury of 0.09% with UMR-PRU.

The molar flows of mercury in all streams present in the plant were examined for both models and they are shown in Table 4.6. Then, the recovery of mercury in the first three-phase separator with both models was calculated, which is presented in Table 4.7. Furthermore, using the results of the simulation, the recovery of Hg in the outlet streams was calculated with respect to the inlet feed (

Table **4.8**).

***Table 4.6** - Molar flows of mercury in all streams present in the plant as obtained with SRK-Twu and UMR-PRU models*

	Hg Mole Flow (kgmol/h)	
Stream	**SRK-Twu**	**UMR-PR**
Inlet Feed	4,95E-08	4,95E-08
Gas	2,25E-08	3,36E-08
C1	3,30E-08	2,73E-08
C9	3,61E-08	3,08E-08
Water	1,31E-10	6,60E-11

G1	4,96E-09	9,09E-09
G2	2,63E-08	3,53E-08
Water2	2,06E-13	1,66E-13
Export Condensate	2,61E-08	1,72E-08
G3	2,43E-08	3,28E-08
G6	1,01E-08	1,36E-08
G10	7,04E-09	1.03E-08
G14	2,34E-08	3,25E-08
Fuel Gas	2,34E-08	3,25E-08
Export Gas	2,34E-08	3,22E-08

Table 4.7 *– Hg recovery in the first three-phase separator for the Vapor, Liquid and Water Phases of the simulations with SRK-Twu and UMR-PRU*

	Hg Recovery		
	Vapor Phase	**Liquid Phase**	**Water Phase**
SRK-Twu	40,4%	59,4%	0,23%
UMR-PRU	55,1%	44,8%	0,11%

Table 4.8 *– Recovery of mercury in the outlet streams calculated with respect to the inlet feed of the simulations with SRK-Twu and UMR-PRU models*

	Hg Recovery	
Outlet Stream	**SRK-Twu**	**UMR-PR**
Export Gas	47,15%	65,13%
Export Condensate	52,71%	34,65%
Water	0,26%	0,13%

As regards the comparison between the thermodynamic models, it was observed that they give opposite results for the concentration of mercury in the streams. It is possible to see that mercury prefers the liquid phase with the SRK-Twu model and, on the contrary, UMR-PRU predicts slightly higher mercury recovery in the vapor phase. What concerns

the distribution of mercury in the aqueous phase, the results obtained are reasonable for both models, because, as already discussed, mercury has a slight solubility in water [1]. Besides, the results of the recovery of mercury in the outlet streams follow the same trend as in the first three-phase separator. In fact, this is the most important separator because it dictates the distribution of the mercury in the whole plant.

Although the tendency of mercury to distribute itself in the various phases is opposite between the two models, it is not possible to establish which one is correct, because no experimental data were available in order to compare them with the model results. It should be noted that the streams treated in the plant are multicomponent systems, so, apart from mercury, they contain other components as well. The distributions obtained for these compounds are also different between the models, as shown by the different values of the total mole flowrates in the first three-phase separator, presented in

Table **4.9**, particularly for the vapor and liquid phases.

Table 4.9 *– Total Mole Flowrates in the first three-phase separator obtained by the simulations with SRK-Twu and UMR-PRU*

	Total Flowrates (kgmol/h)		
	Vapor Phase	**Liquid Phase**	**Aqueous Phase**
SRK-Twu	32208	6205	12610
UMR-PRU	32305	6346	12620

4.3.1 Evaluation of the models based on K-value analysis

In addition to the analysis made before, the K-values were examined. This analysis is necessary to better understand how the models predict mercury distribution between the vapor, liquid and aqueous phases. Below, the results of the analysis for the all equipment present in the plant are shown in Table 4.10.

***Table 4.10** – K values for the Organic Phase and Aqueous Phase of all the equipment of the simulations with SRK-Twu and UMR-PRU*

	SRK-Twu		**UMR-PRU**	
Equipment (Operating Conditions)	**K_{org}**	**K_{aq}**	**K_{org}**	**K_{aq}**
V-100 (88,6 °C; 87 bar)	0,13	67,5	0,24	199
V-101 (105 °C; 26 bar)	0,35	-	0,66	-
V-102 (72,8 °C; 2,1 bar)	1,71	1789	3,52	1941
V-103 (25 °C; 1,6 bar)	4,19	-	2,04	-
V-104 (25 °C; 7 bar)	0,67	-	0,60	-
V-105 (25°C; 25 bar)	0,29	-	0,21	-
V-106 (26 °C; 86 bar)	0,18	-	0,12	-
V-107 (25 °C; 84,2 bar)	0,14	-	0,13	-

Observing the results of K values, it is possible to see that they are in accordance with the results for the recovery. In the first three-phase separator, (V-100), the K value for the organic phase with UMR-PRU is higher than the one with SRK-Twu. This confirms the fact that mercury partitions more preferably to the vapor phase according to UMR-PRU as compared with SRK-Twu. In the series of equipment V-103, V-104, V-105, the temperature is kept constant and the pressure increases gradually. In this case, K values decrease, and this means that mercury prefers the organic phase because the liquid fraction increases with increasing pressure. What concerns the aqueous phase, it should be noted that the values obtained with SRK-Twu are higher than the values obtained with UMR-PRU. This means that the amount of mercury in the aqueous phase with SRK-Twu is higher than the quantity predicted with UMR-PRU.

Afterward the temperature of the first three-phase separator was changed in order to observe the dependence of K variables from this parameter. At the beginning the temperature was equal to 88.6°C and then it was increased to 95°C and 100°C, while the pressure was kept constant. The trends of K values obtained for the Aqueous and Organic phase of the equipment V-100 are shown in Figure 4.3 and Figure 4.4 respectively.

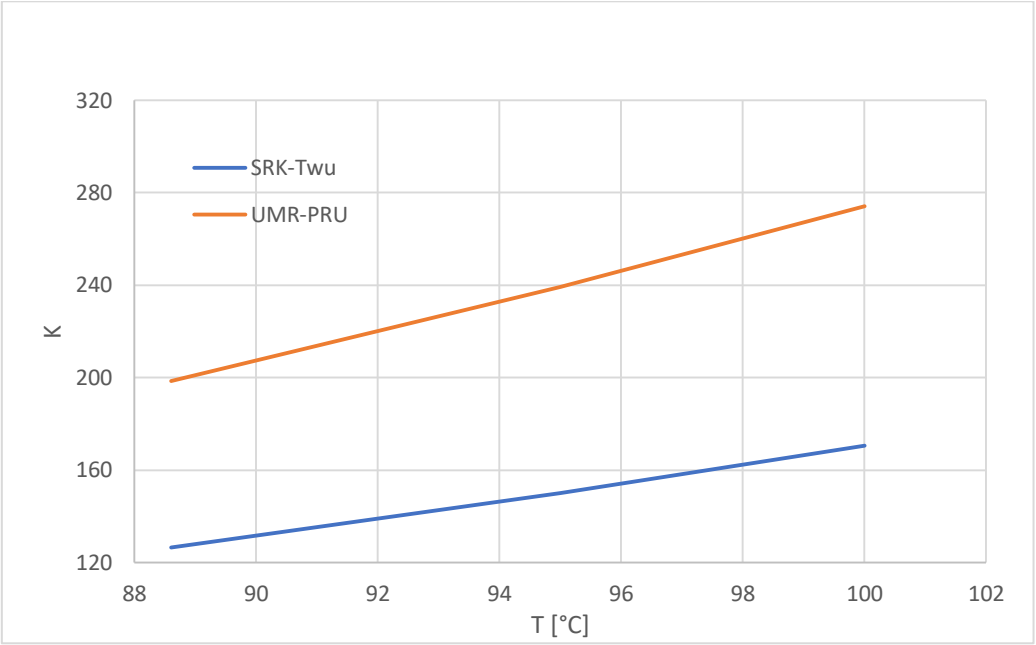

Figure 4.3 – *K values for Hg of the first three-phase separator for the aqueous phase in the simulations with SRK-Twu and UMR-PRU*

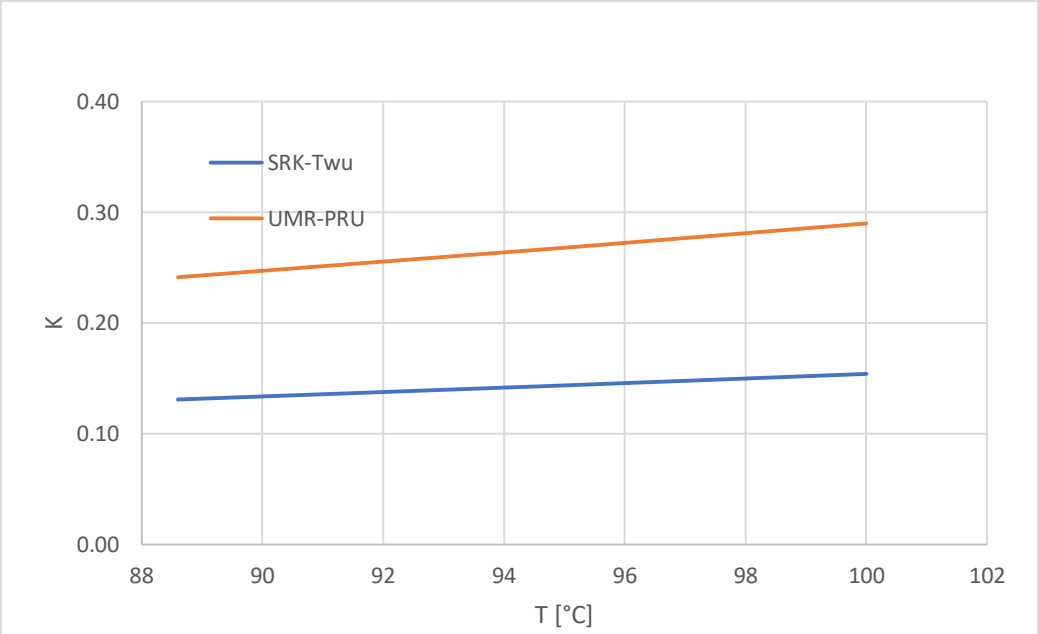

Figure 4.4 *– K values for Hg in the first three-phase separator for the organic phase in the simulations with SRK-Twu and UMR-PRU*

By observing the charts, it is possible to see that K values increase with increasing temperature, both for the aqueous and the organic phases. This was expected since solubility of Hg increases in the vapor phase when temperature increases. Even if the values are different, the trends for both models are the same.

4.4 Sensitivity Analysis

The second part of this work concerns the sensitivity analysis, which took place in order to examine how the partitioning of mercury is affected by the composition of the inlet feed and some operating conditions of the plant, such as temperature and pressure, and to see how the distributions of the other components in the outlet streams are also affected.

The sensitivity analysis consists of two parts:

- Modification of the Inlet Feed
    - Hg content increase to 1 ppb and 1 ppm
    - C_{7+} flowrate increase by 50%, 100%, 200%
    - Water content set to 10% and 50% per mol

- Modification of the operating conditions at the first three-phase separator
    - Temperature decrease to 30, 50, 70 °C
    - Pressure decrease to 50 and 70 bar

Sensitivity analysis was carried out for both thermodynamic models, i.e. SRK-Twu and UMR-PRU, and the obtained results were compared. During all simulations, the mass balance of Hg was monitored, because it is very difficult to be satisfied. In order to achieve that and not to have any production or loss of mercury higher than 1%, the sensitivities of the recycles were reduced.

For each analysis, the other conditions are set always to the base initial values. What concerns the mercury content in the inlet feed, after its modification in the first analysis, for the others analysis it was set to 1 ppb in order to better understand the behavior of mercury since the initial composition of 1 ppt is too small.

4.4.1 Modification of the Inlet Feed

4.4.1.1 Hg content

At first the effect of the increase of mercury content present in the inlet feed on its partitioning was investigated. At the beginning, the molar composition of mercury was 1 ppt, then it was changed in 1 ppb and in 1 ppm. The recovery of mercury in the first three phase separator was checked, for both thermodynamic models, and the data are shown in Table 4.11. Furthermore, the recovery of mercury in the outlet streams of the plant was also checked as shown in

Table **4.12**.

Table 4.11 *– Recovery of Hg in the first three-phase separator for various concentrations of mercury in the Inlet Feed, as obtained with SRK-Twu and UMR-PRU*

	Hg recovery					
	Vapor Phase		**Liquid Phase**		**Aqueous Phase**	
	SRK-Twu	**UMR-PRU**	**SRK-Twu**	**UMR-PRU**	**SRK-Twu**	**UMR-PRU**
1 ppt	40,4%	55,1%	59,4%	44,8%	0,23%	0,11%
1 ppb	40,4%	55,1%	59,4%	44,8%	0,23%	0,11%
1 ppm	40,4%	55,1%	59,4%	44,8%	0,23%	0,11%

***Table 4.12** – Recovery of Hg in the outlet streams for various concentrations of Hg in the Inlet Feed, as obtained with SRK-Twu and UMR-PRU*

	Hg Recovery					
Outlet Streams	**1 ppt of Hg**		**1 ppb of Hg**		**1 ppm of Hg**	
	SRK-Twu	**UMR-PRU**	**SRK-Twu**	**UMR-PRU**	**SRK-Twu**	**UMR-PRU**
Export Gas	47,15%	65,13%	47,08%	64.96%	46.99%	64,92%
Export Condensate	52,71%	34,65%	52,17%	34,41%	51,93%	34,47%
Water	0,26%	0,13%	0,26%	0,13%	0,26%	0,13%

Observing the results, it is possible to see that if the initial composition of mercury increases, the distribution of mercury does not change in the first three-phase separator significantly. In this separator, according to the SRK-Twu model, more mercury is found in the liquid phase with respect to the vapor and the aqueous phases. On the other hand, with the UMR-PRU model, the vapor phase is richer in mercury as compared with the liquid and aqueous phases. The trends of this analysis are the same as those seen before in the evaluation of the models. This first separator is decisive for the final recovery of mercury. In fact, with SRK-Twu model it was calculated that most of the mercury is recovered in the Export Condensate, while with UMR-PRU most of the mercury is found in the export gas. This is observed for all different inlet feed compositions of mercury.

Mercury content in the inlet feed does not affect the recovery. So, it follows the normal distribution in the various phases.

By inserting a molar composition of mercury in the Inlet Feed equal to 1 ppb, the mercury mass balance closes with a deviation of about 0.50% for both SRK-Twu model and UMR-PRU model. Instead, by using a molar composition of 1 ppm there is a deviation of 0.82% with SRK-Twu and 0.48% with UMR-PRU.

In order to have simulation results directly comparable with each other, the concentration of mercury in the Export Gas was expressed in ng/Sm^3 and it is shown in

Table 4.13. The Standard Conditions are 15°C and 1 atm. Comparing the two thermodynamic models, UMR-PRU predicts a higher Hg content than SRK-Twu and this is due to the fact that mercury prefers to go to the gas phase according to UMR-PRU model, as previously discussed. The specification in product gas established from Equinor is 10 ng/Sm^3 [21]. Therefore, when the molar composition of mercury in the inlet feed is 1 ppm, the specification is not satisfied.

***Table 4.13** – Mercury concentration in ng/Sm^3 in the Export Gas for various molar composition of mercury in the Inlet Feed as obtained with SRK-Twu and UMR-PRU*

	Hg concentration (ng/Sm^3)	
Concentration of Hg in the Inlet Feed	**SRK-Twu**	**UMR-PRU**
1 ppt	6,03E-05	8,32E-05
1 ppb	0,06	0,08
1 ppm	60,1	82,9

Besides, the distributions of all the other components in the Export Gas and in the Export Condensate were observed while changing the concentration of mercury in the inlet feed. The components were divided in: (i) Light components, including C1, C2 and C3 fractions, (ii) Heavy components, including C4 and C5 fractions, and (iii) Pseudo components. As regards the comparison between the thermodynamic models, it is observed that both models give similar results for the distributions of the components with no significant differences between them. This means that the distributions of the components are not affected by the content of the mercury.

The results obtained with 1 ppt of Hg in the Inlet Feed are shown in the charts presented in

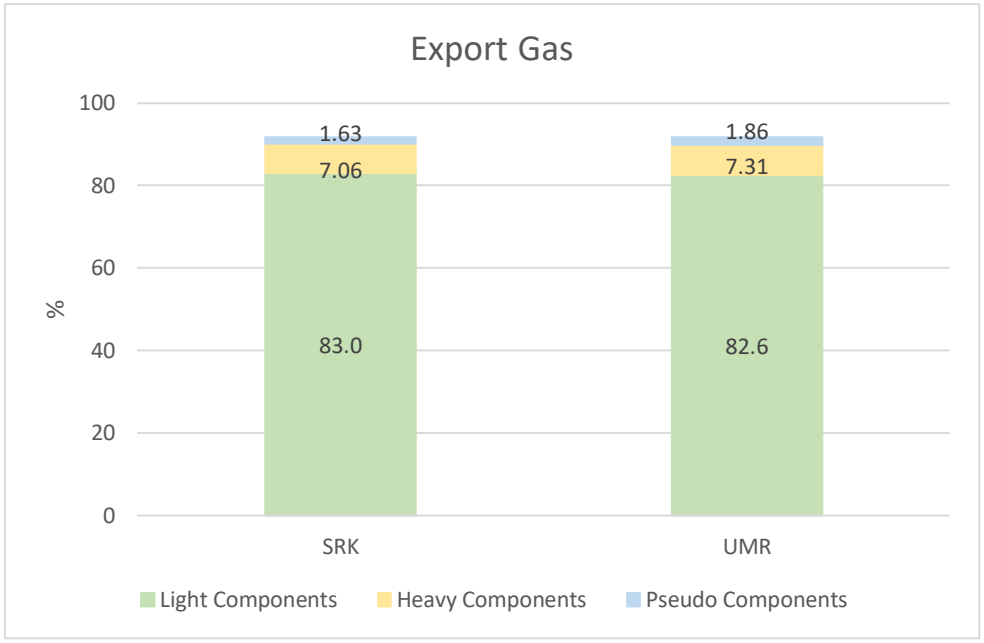

Figure **4.5** and Figure 4.6. The distributions with 1 ppb and 1 ppm in the Inlet Feed are the same.

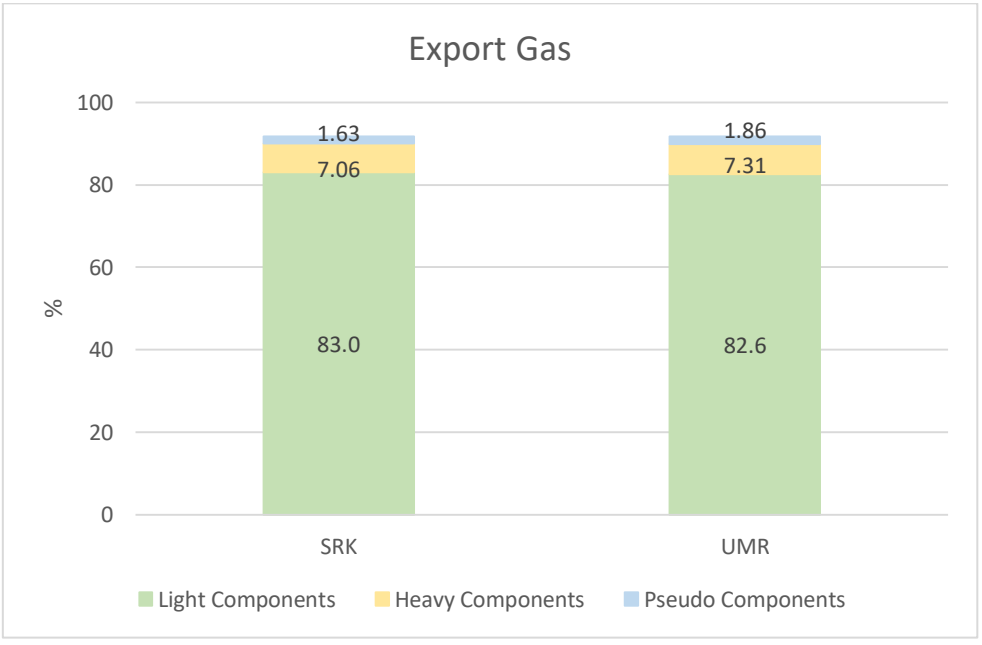

***Figure 4.5** - Distribution of Light, Heavy and Pseudo Components in the Export Gas for 1 ppt of Hg in the Inlet Feed as obtained with SRK-Twu and UMR-PRU*

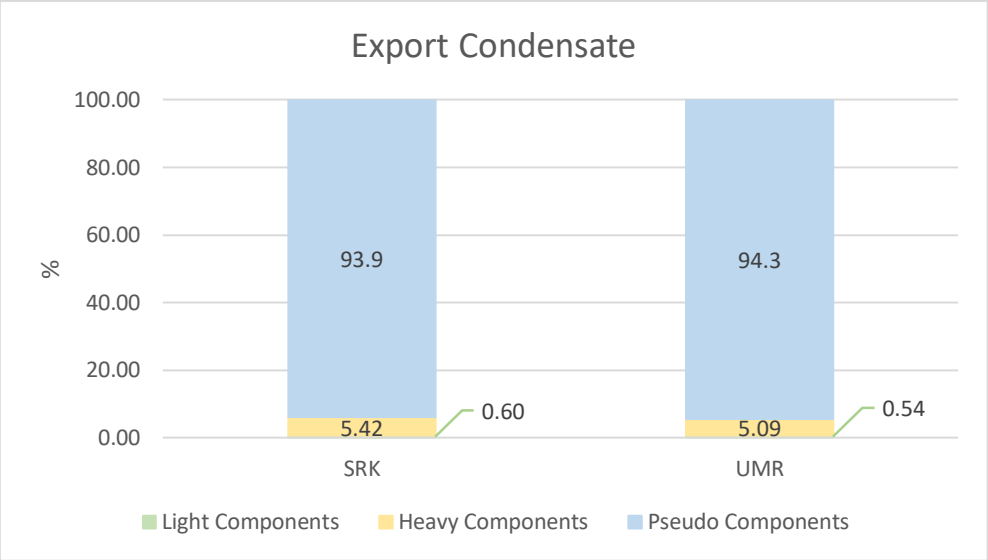

Figure 4.6 *- Distribution of Light, Heavy and Pseudo Components in the Export Condensate for 1 ppt of Hg in the Inlet Feed as obtained with SRK-Twu and UMR-PRU*

Furthermore, the distributions of the components in the two water streams present in the plant were also checked, but no considerable differences were found. The composition percentage of the other components in the outlet streams with respect to the total flowrate is very close to zero, because mainly water is removed from the two three-phase separators in the stabilization region. For this reason, charts regarding the water were not included in the work. Besides, mercury has a very low solubility in water, so the quantity of mercury in the aqueous phase is almost the same and this does not affect the distributions of the other components in the water streams.

4.4.1.2 C_{7+} flowrates

The second analysis is made on the C_{7+} flowrates. The flowrates of the Pseudo components in the inlet feed were increased by 50%, 100% and 200% with respect to the initial flowrates. The recovery of mercury in the first three-phase separator was checked, and it is shown in Table 4.14 - Recovery of Hg in the first three-phase separator by increasing C_{7+} Flowrate in the inlet feed, as obtained with SRK-Twu and UMR-PRU. Furthermore, the recovery of Hg in the outlet streams was monitored and the values are

shown in Table 4.15. The gradual increase of the C_{7+} flowrates leads more mercury in the liquid phase with respect to the vapor and aqueous phases according to both models.

In accordance with the results of the first three-phase separator, according to SRK-Twu, most of the mercury is in the Export Condensate and its recovery increases with increasing C_{7+} flowrates. What concerns UMR-PRU, at the beginning mercury is more in the Export Gas but then an increase of the mercury concentration in the Export Condensate is observed with increasing C_{7+} flowrates, following the same trend of SRK-Twu. This is due to the fact that the liquid fraction increases with increasing C_{7+} flowrates and this means that the amount of mercury in the liquid phase is higher than the base case. In fact, as previously discussed, the solubility of mercury in liquid hydrocarbons increases with increasing number of carbon atoms [10].

Table 4.14 *- Recovery of Hg in the first three-phase separator by increasing C_{7+} Flowrate in the inlet feed, as obtained with SRK-Twu and UMR-PRU*

	Hg recovery					
	Vapor Phase		**Liquid Phase**		**Aqueous Phase**	
Increase C7+ Flowrate	**SRK-Twu**	**UMR-PRU**	**SRK-Twu**	**UMR-PRU**	**SRK-Twu**	**UMR-PRU**
Basis	40,4%	55,1%	59,4%	44,8%	0,23%	0,11%
+50%	30,8%	44,8%	69,1%	55,1%	0,19%	0,09%
+100%	24,6%	37,4%	75,2%	62,5%	0,15%	0,08%
+200%	11,4%	19,0%	88,5%	80,9%	0,08%	0,05%

Table 4.15 *- Partitioning of Hg in the outlet streams by increasing C_{7+} Flowrate in the inlet feed, as obtained with SRK-Twu and UMR-PRU*

Increase in C7+ Flowrate

	Basis		+50%		+100%		+200%	
Outlet Stream	**SRK-Twu**	**UMR-PRU**	**SRK-Twu**	**UMR-PRU**	**SRK-Twu**	**UMR-PRU**	**SRK-Twu**	**UMR-PRU**
Export Gas	47,15%	65,13%	40,6%	60,2%	36,9%	56,7%	28,0%	48,1%
Export Condensate	52,71%	34,65%	58,2%	39,7%	62,9%	43,1%	71,7%	51,8%
Water	0,26%	0,13%	0,20%	0,11%	0,17%	0,09%	0,09%	0,05%

Besides, the distributions of all other components in the outlet streams were also checked by changing the C_{7+} flowrate. These distributions are shown in

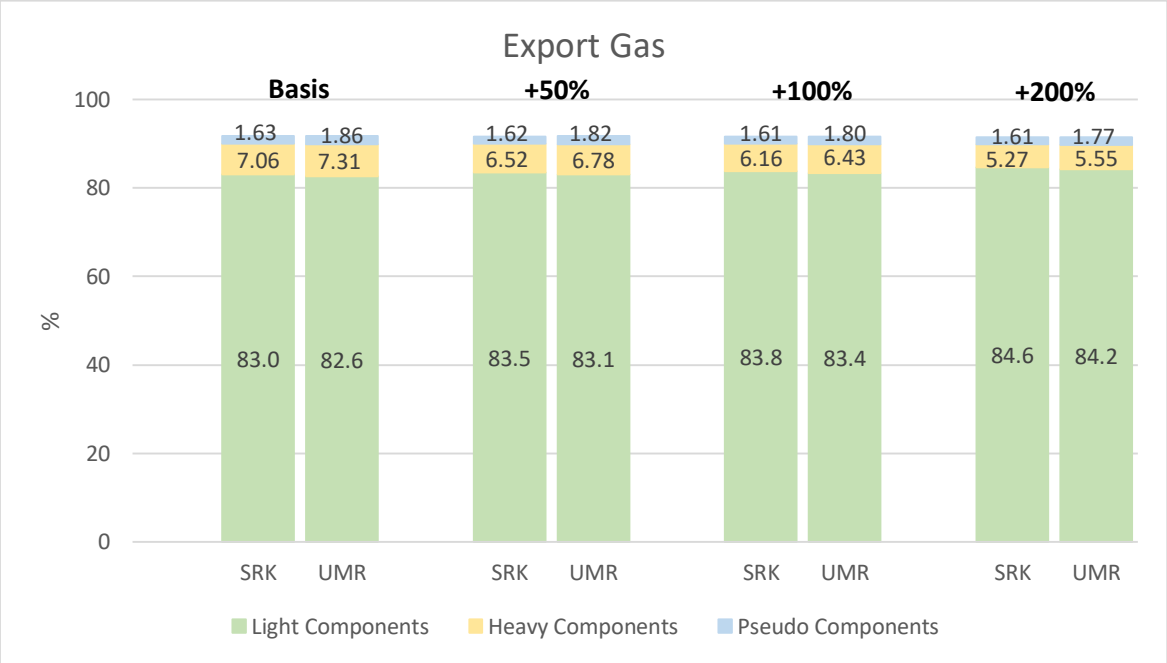

Figure **4.7** and Figure 4.8.

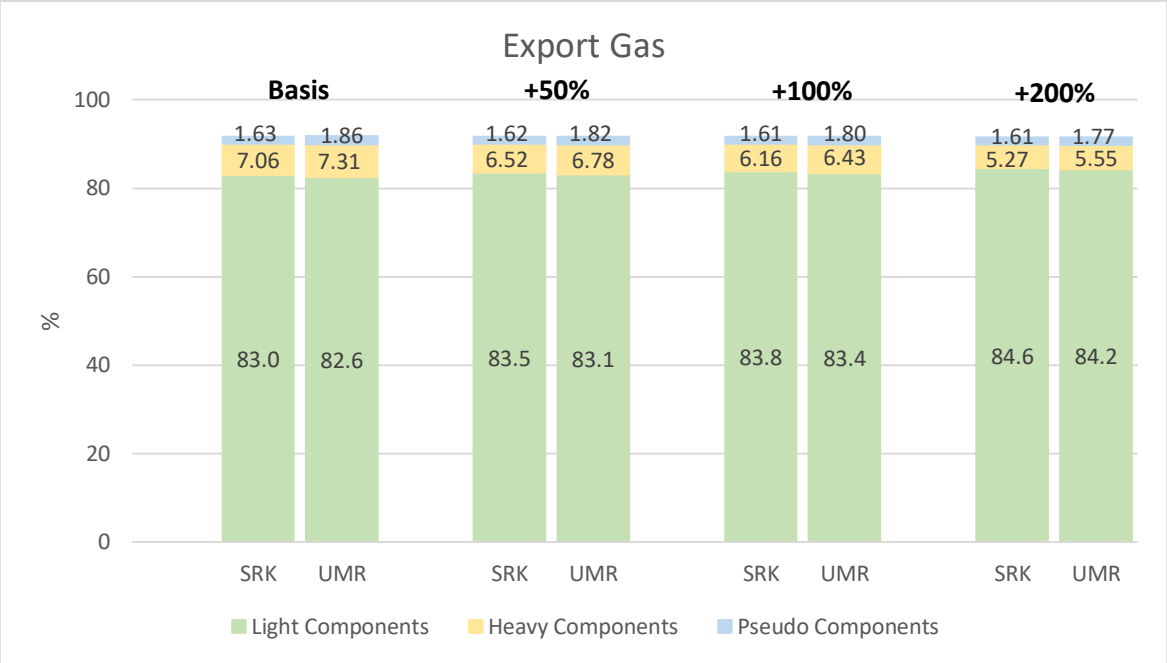

Figure 4.7 *- Distribution of Light, Heavy and Pseudo Components in the Export Gas by increasing the C_{7+} Flowrate in the inlet feed, as obtained with SRK-Twu and UMR-PRU*

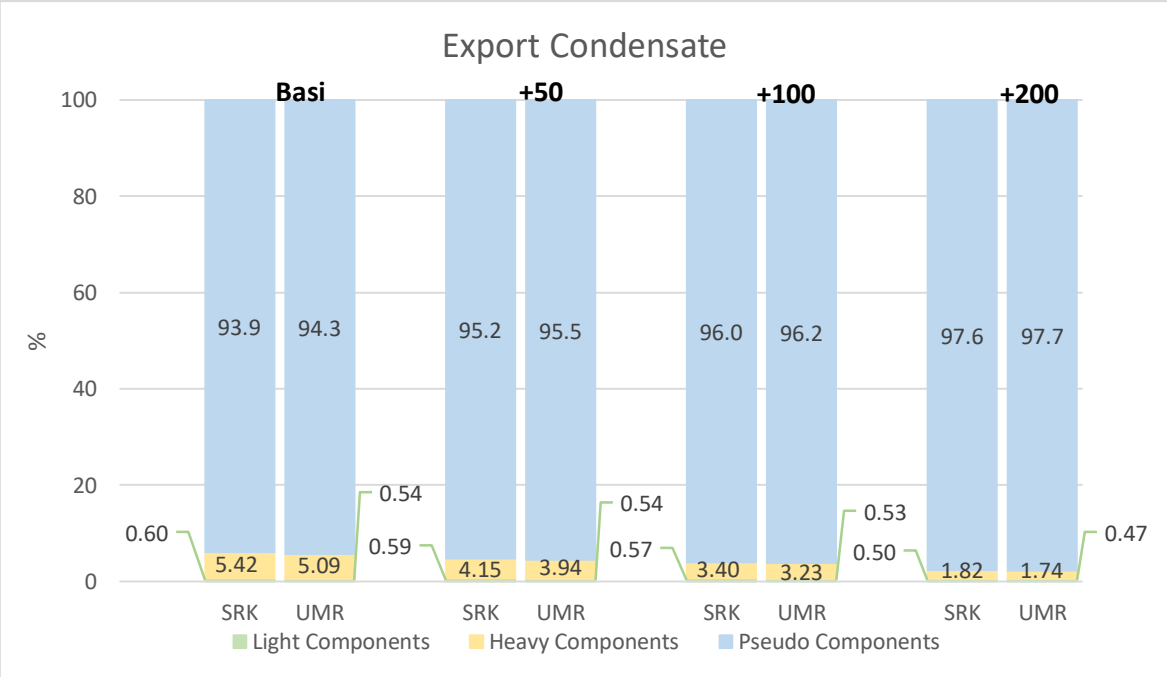

Figure 4.8 *- Distribution of Light, Heavy and Pseudo Components in the Export Condensate by increasing the C_{7+} Flowrate in the inlet feed, as obtained with SRK-Twu and UMR-PRU*

Observing the chart for the Export Condensate, when C_{7+} flowrate increases, the Pseudo components increase as well, as expected. Instead, Heavy components in the Export Condensate decrease in order to redistribute the percentage. What concerns the content of Light components, they do not change in the Export Condensate.

In the Export Gas there is an increase of the Light components and a decrease of the Heavy and Pseudo components. Obviously, Pseudo components decrease because they go mainly in the liquid phase and Light components have to increase in order to cover the space. Also, in this case, the percentages of all components in the two water streams are close to zero and there are no significant changes in the distributions, because the stream is comprised almost entirely of water.

Comparing the two thermodynamic models, it is possible to say that their results are qualitatively similar. Thus, even if the values are different, the trends are the same for both thermodynamic models.

4.4.1.3 Water content

The last analysis made on the inlet feed is the modification of the water content. At the beginning the molar composition was 25%, that is a significant amount of water. It was decreased to 10% and then increased to 50%. As the other modifications, the partitioning of mercury in the first three-phase separator was examined and it is shown in Table 4.16. In addition, the values of the recoveries for the outlet streams are shown in

Table **4.17**. By increasing the water content, it is observed that the recoveries of mercury in the vapor and liquid phase decrease slightly for both models, while the recovery of mercury in the aqueous phase increases. Since solubility depends only from temperature and pressure and these parameters are fixed, if the aqueous fraction increases, also the amount of the solute has to increase in order to maintain the same solubility. Nevertheless, the amount of mercury in the aqueous phase continues to be very small because mercury has a very low solubility in water [1].

In accordance with the results for the first three-phase separator, the recoveries of mercury in Export Gas and Export Condensate decrease while the recovery of mercury in the Water stream increases, for both models. In the plant two water streams are present

but, for simplicity, they are added together and represented in the tables as a unique stream.

Table 4.16 *- Recovery of Hg in the first three-phase separator by changing water content in inlet feed, as obtained with SRK-Twu and UMR-PRU*

	Hg Recovery					
	Vapor Phase		**Liquid Phase**		**Aqueous Phase**	
Water Content	**SRK-Twu**	**UMR-PRU**	**SRK-Twu**	**UMR-PRU**	**SRK-Twu**	**UMR-PRU**
25% (basis)	40,4%	55,1%	59,4%	44,8%	0,23%	0,11%
10%	40,5%	55,2%	59,5%	44,8%	0,07%	0,03%
50%	40,2%	55,0%	59,1%	44,7%	0,68 %	0,32%

Table 4.17 *- Partitioning of Hg in the outlet streams by changing water content in inlet feed, as obtained with SRK-Twu and UMR-PRU*

	Water Content					
	25% (basis)		**10%**		**50%**	
Outlet Stream	**SRK-Twu**	**UMR-PRU**	**SRK-Twu**	**UMR-PRU**	**SRK-Twu**	**UMR-PRU**
Export Gas	47,15%	65,13%	47,24%	65,20%	46,80%	64,97%
Export Condensate	52,71%	34,65%	52,68%	34,72%	52,18%	34,65%
Water	0,26%	0,13%	0,08%	0,04%	0,76%	0,39%

In Figure 4.9 and Figure 4.10 the results of the distributions for all components in the outlet streams are shown.

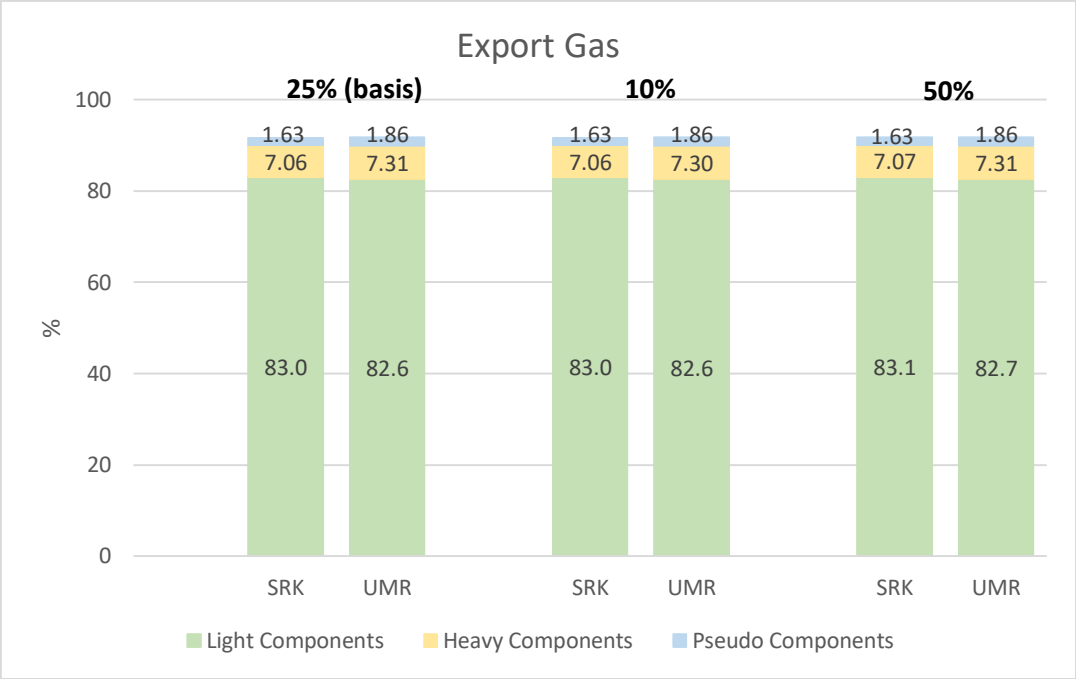

Figure 4.9 *- Distribution of Light, Heavy and Pseudo Components in the Export Gas by changing water content in inlet feed, as obtained with SRK-Twu and UMR-PRU*

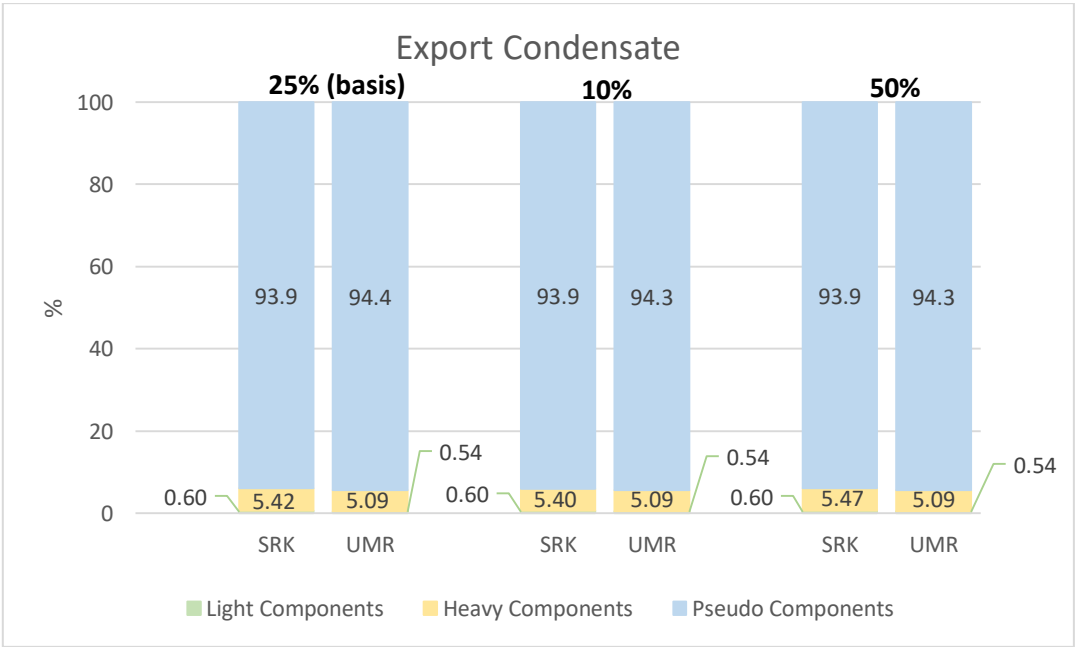

Figure 4.10 *- Distribution of Light, Heavy and Pseudo Components in the Export Condensate by changing water content in inlet feed, as obtained with SRK-Twu and UMR-PRU*

By changing water content in the inlet feed, the distributions of all other components in the Export Gas and Export Condensate are not practically affected. In fact, it was shown that the two three-phase separators remove almost the total amount of water present in the feed, even if it increases. In addition, there is the Component Splitter in the final part of the flowsheet that removes the remaining water present in gas. So, the water fraction in the outlet streams is always the same and the distributions of the components do not have reason to change.

Even in this case, the mole fractions of the components in the two water streams are close to zero and there are no significant changes when the water content increases.

4.2.2 Modification of the operating conditions at the first three-phase separator

4.2.2.1 Temperature

The second part of the sensitivity analysis consists of the modification of the operating conditions at the first three-phase separator. The first analysis is made on the temperature of this separator, which at the initial scenario was 88,6 °C. Then it was decreased to 70°C, 50°C and 30°C.

In Table 4.18, the results for the recovery of mercury in the vapor, liquid and aqueous phase in this separator are presented. In addition, in Table 4.19, the results for the recovery of mercury in the three outlet streams are shown.

Table 4.18 *- Recovery of Hg in the first three-phase separator by decreasing the temperature at first three-phase separator, as obtained with SRK-Twu and UMR-PRU*

	Hg recovery					
	Vapor Phase		**Liquid Phase**		**Aqueous Phase**	
Temperature	**SRK-Twu**	**UMR-PRU**	**SRK-Twu**	**UMR-PRU**	**SRK-Twu**	**UMR-PRU**
88,6°C (basis)	40,5%	55,1%	59,4%	44,8%	0,13%	0,11%
70°C	31,9%	44,4%	67.9%	55,5%	0,18%	0,17%
50°C	23,1%	32,3%	76,6%	67,5%	0,28%	0,28%
30°C	15,4%	21,1%	84,1%	78,5%	0,45%	0,49%

Table 4.19 - *Partitioning of Hg in the outlet streams by decreasing the temperature at first three-phase separator, as obtained with SRK-Twu and UMR-PRU*

	Temperature							
	88,6 °C (basis)		**70 °C**		**50 °C**		**30 °C**	
Outlet Stream	**SRK-Twu**	**UMR-PRU**	**SRK-Twu**	**UMR-PRU**	**SRK-Twu**	**UMR-PRU**	**SRK-Twu**	**UMR-PRU**
Export Gas	47,26%	65,13%	44,45%	62,81%	40,80%	58,98%	37,15%	54,82%
Export Condensate	52,41%	34,65%	55,63%	36,76%	58,58%	41,06%	63,59%	44,87%
Water	0,14%	0,13%	0,19 %	0,18%	0,28%	0,28%	0,45%	0,49%

It is possible to observe that, by decreasing the temperature, the amount of mercury in the vapor phase decreases, because vapor fraction decreases as well. The results of the two thermodynamic models follow the same trends. It should be noted that the differences between SRK-Twu and UMR-PRU, in the analysis concerning mercury, consist always in its distribution among the vapor and the liquid phase. In fact, comparing the results of the two thermodynamic models for the same temperature, it is possible to observe that UMR-PRU still predicts higher amount of mercury in the vapor phase as compared with SRK-Twu. On the other hand, the quantity of mercury in the liquid phase is always higher with SRK-Twu than UMR-PRU.

What concerns the aqueous phase, the recovery of mercury increases for both models.

The recoveries of mercury in the outlet streams follow the same trend with the partitioning in the first three-phase separator.

The distributions of all other components in the outlet streams are checked and they are presented in **Σφάλμα! Το αρχείο προέλευσης της αναφοράς δεν βρέθηκε.** and Figure 4.12.

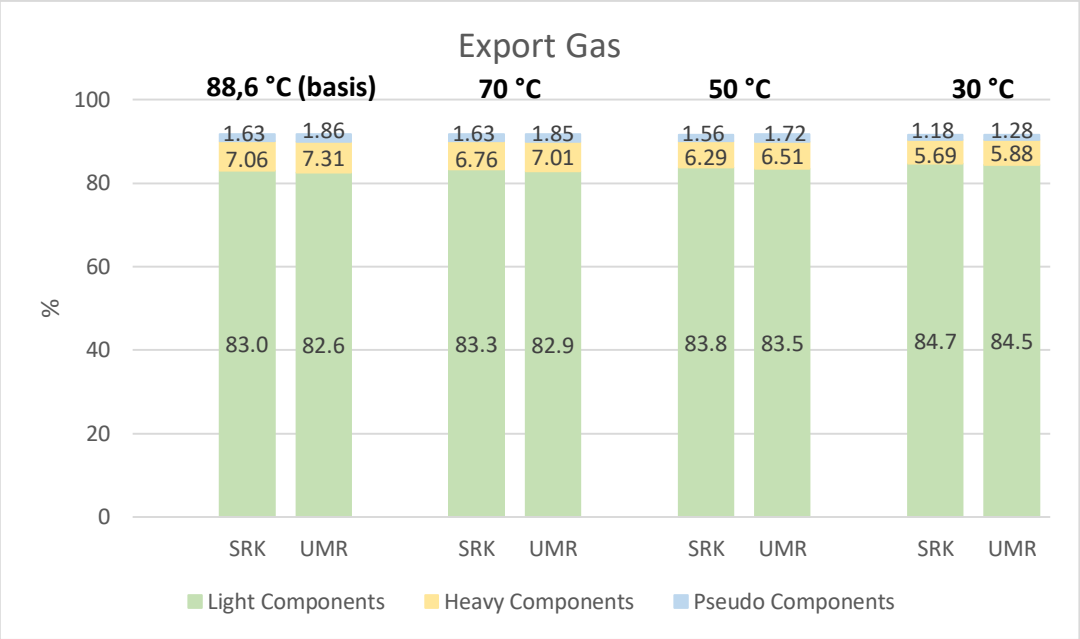

Figure 4.11 *– Distribution of Light, Heavy and Pseudo Components in the Export Gas by decreasing the temperature at first three-phase separator, as obtained with SRK-Twu and UMR-PRU*

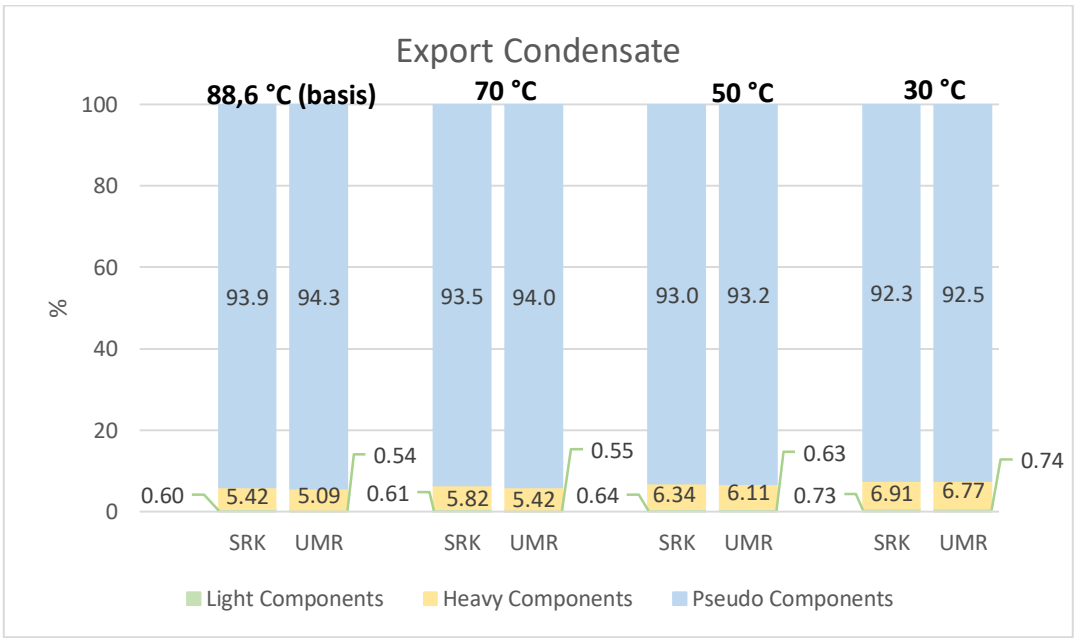

Figure 4.12 *- Distribution of Light, Heavy and Pseudo Components in the Export Condensate by decreasing the temperature at first three-phase separator content, as obtained with SRK-Twu and UMR-PRU*

In the Export Condensate it is possible to see an increase of the Heavy components and a slightly increase of the Light components, because by decreasing the temperature, also the vapor pressure of the components decreases. The Pseudo components decrease in order to redistribute the percentages in the stream. On the other hand, in the Export Gas there is a decrease of the Heavy components and Pseudo components, because they go in the liquid phase for the same reason of the decrease of the vapor pressure. Furthermore, it is possible to observe an increase of the Light components in order to cover the space left by the other two groups of components.

Even in this case, the mole fractions of mercury in the two water streams are close to zero and there are no significant differences. The results between the two thermodynamic models are close and they follow the same trends.

4.2.2.2 Pressure

The last analysis is made on the pressure at the first three-phase separator. At the beginning it was 87 bar, then it was changed to 70 bar and 50 bar. Since the vapor stream from the first three-phase separator is the gas train of the plant, it is necessary to change the pressure also in the last two separators, that are the equipment V-106 and V-107, according to each pressure.

The values about the recovery of mercury in the first three-phase separator are shown in Table 4.20. In

Table **4.21** the simulation results regarding the partitioning of mercury in the outlet streams with changing the pressure are presented.

***Table 4.20** – Recovery of Hg in the first three-phase separator by decreasing the pressure at first three-phase separator, as obtained with SRK-Twu and UMR-PRU*

	Hg recovery					
	Vapor Phase		**Liquid Phase**		**Aqueous Phase**	
Pressure	**SRK-Twu**	**UMR-PRU**	**SRK-Twu**	**UMR-PRU**	**SRK-Twu**	**UMR-PRU**
87 bar (basis)	40,4%	55,1%	59,4%	44,8%	0,23%	0,11%
70 bar	44,1%	59,1%	55,7%	40,8%	0,22%	0,11%

50 bar	50,9%	66,0%	48,9%	33,9%	0,20%	0,11%

Table 4.21– *Partitioning of Hg in the outlet streams by decreasing the pressure at first three-phase separator, as obtained with SRK-Twu and UMR-PRU*

	Pressure					
	87 bar (basis)		**70 bar**		**50 bar**	
Outlet Stream	**SRK-Twu**	**UMR-PRU**	**SRK-Twu**	**UMR-PRU**	**SRK-Twu**	**UMR-PRU**
Export Gas	47,15%	65,13%	48,37%	66,02%	52,66%	69,85%
Export Condensate	52,71%	34,65%	51,32%	33,84%	47,16%	30,01%
Water	0,26%	0,13%	0,25 %	0,14%	0,23%	0,13%

By decreasing the pressure there is an increase of the amount of mercury in the vapor phase, a decrease in the liquid phase and also a slightly decrease in the aqueous phase, for both thermodynamic models used. These trends are reasonable because, when pressure decreases, an increase of the vapor fraction occurs.

The comparison of the two models leads to the same observations as before. In fact, by observing the amount of mercury present in the vapor phase for the same value of pressure, it is possible to note that UMR-PRU predicts a quantity higher than SRK-Twu. On the contrary, the amount of mercury observed in the liquid phase is higher with SRK-Twu than UMR-PRU.

It should be noted that the quantity of mercury solubilized in the aqueous phase is higher with SRK-Twu as compared with UMR-PRU, regardless the value of pressure. These results are in accordance with the results seen in the analysis of the K values presented in Table 4.10.

In Figure 4.13 and Figure 4.14 the results about the distributions of the components in the outlet streams are shown. For the same reason, i.e. due to the increase of the vapor fraction, there is an increase of the Heavy components in the Export Gas. Instead, concerning Light components, they follow a first slightly increasing trend and afterwards a decreasing trend. On the other hand, Pseudo components decrease and this is expected.

Regarding the Export Condensate, there is a decrease of the Light and Heavy components, because they partition in vapor phase. As a consequence, an increase of the Pseudo components occurs in order to cover the space left by the others. The fractions of mercury in water streams are not reported because they are close to zero and there are no important differences.

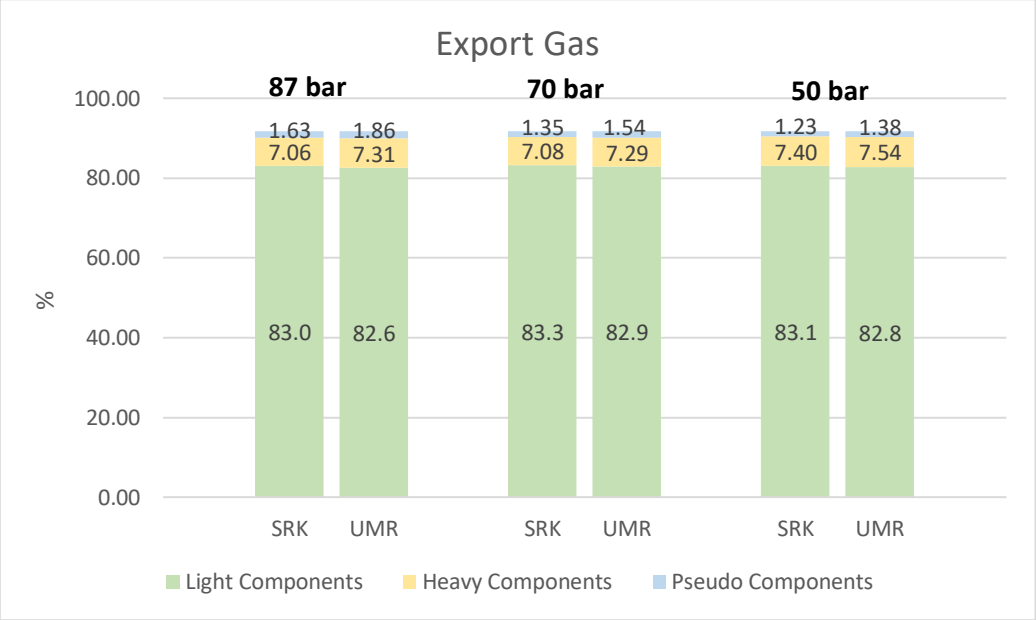

***Figure 4.13** – Distribution of Light, Heavy and Pseudo Components in the Export Gas by decreasing the pressure at first three-phase separator, as obtained with SRK-Twu and UMR-PRU*

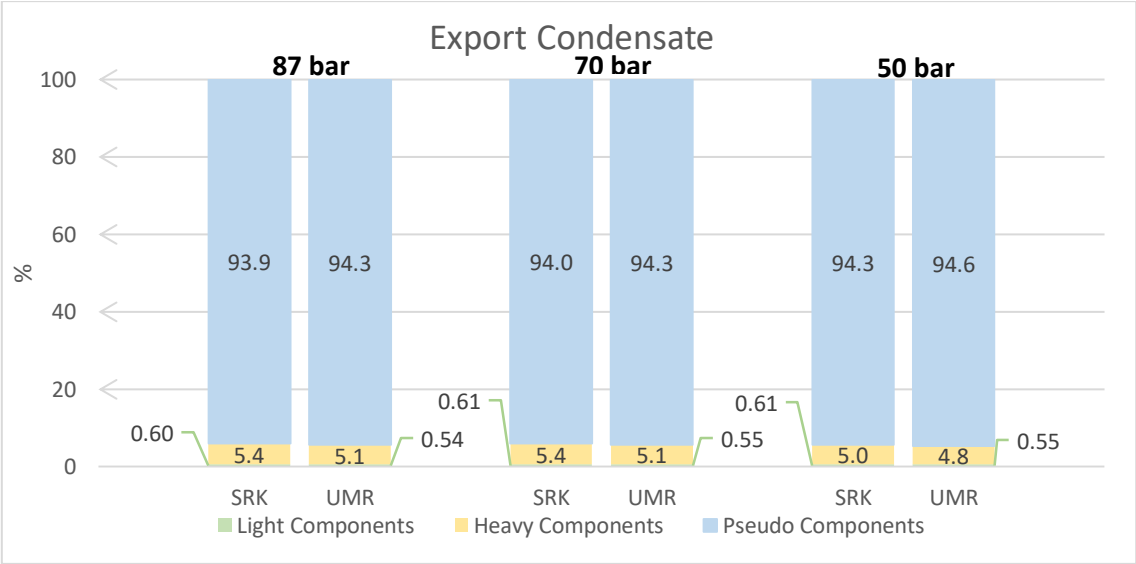

***Figure 4.14** - Distribution of Light, Heavy and Pseudo Components in the Export*

Condensate by decreasing the pressure at first three-phase separator, as obtained with SRK-Twu and UMR-PRU

In addition to the analysis made above, the phase envelopes for the Export Gas were checked. The curves in Figure 4.15 and in Figure 4.16 show phase envelopes for SRK-Twu and for UMR-PRU respectively, both obtained in the base case (87 bar).

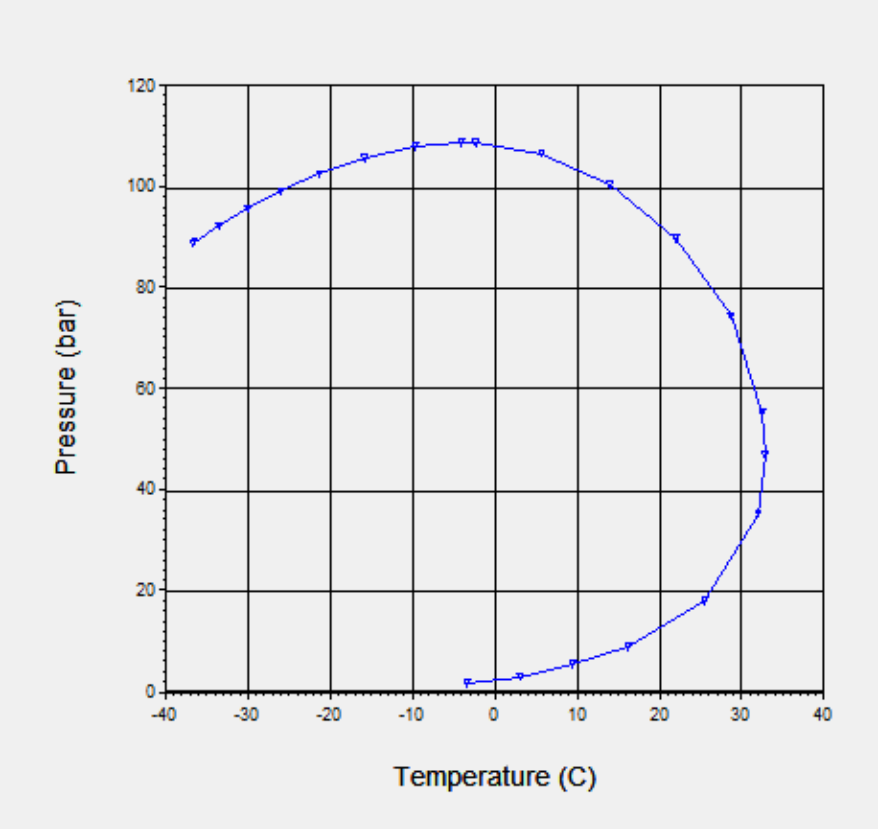

Figure 4.15 *– Phase envelope for the Export Gas as obtained with SRK-Twu in the base case*

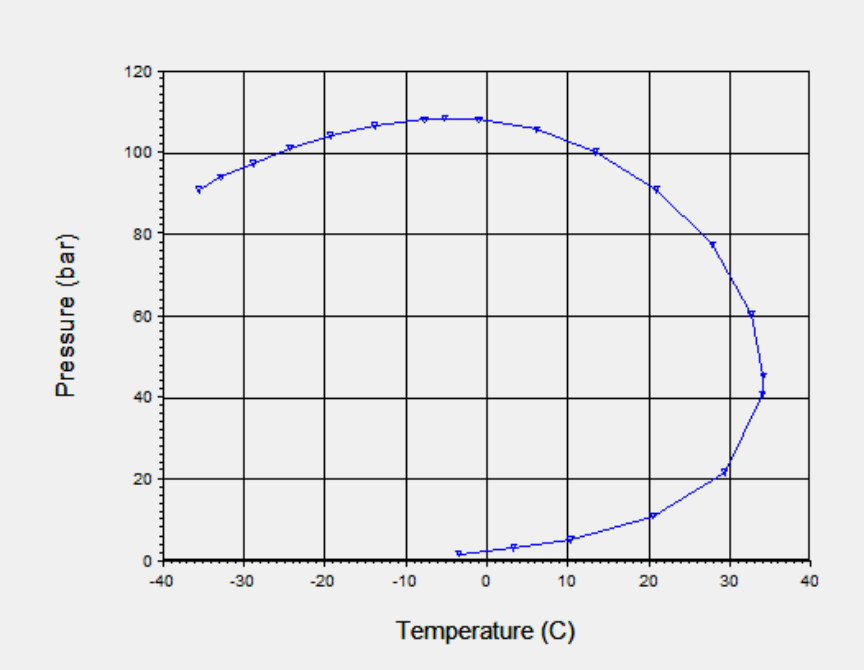

Figure 4.16 *- Phase envelope for the Export Gas as obtained with UMR-PRU in the base case*

In the natural gas operations, the understanding where the operational point is on the phase diagram is important for engineers to avoid design and operating malfunctions. A general knowledge, if not a detailed knowledge, will allow the design engineer and the facilities operator to make intelligent decisions that have significant impact on the profitability of a gas production facility. The practical importance of the phase envelope is for the gas transport in pipelines. In the phase envelope there are two important points that need to be monitored: the cricondenbar and the cricondentherm. Cricondenbar is the maximum pressure above which no gas can be formed regardless of the temperature. Cricondentherm is the temperature above which no liquid can be formed regardless the pressure [22]. The specifications for the "rich gas" transport are 40°C for the max cricondentherm temperature and 105 bar for the max cricondenbar pressure [21].

In addition, the value of the cricondenbar for the Export Gas was checked. In

Table **4.22** the different cricondenbar values for both thermodynamic models are presented, obtained from the simulations by changing the pressure at the first three-phase separator. It is observed that the values are very close between the two models. It should be noted that there is a decrease of the cricondenbar. In fact, it is possible to manipulate

the phase envelope by removing natural gas liquids and also heavy ends (C_{7+}). When the C_{7+} fraction increases, the phase envelope becomes wider [21]. Comparing the results, it can be seen that they are similar, so it was decided not to make any changes in the gas train pressure.

Table 4.22 – *Cricondenbar values for the Export Gas by decreasing the pressure at three phase separator, as obtained with SRK-Twu and UMR-PRU*

	Cricondenbar (bar)	
Pressure	**SRK-Twu**	**UMR-PRU**
87 bar	108,9	108,5
70 bar	105,9	105,6
50 bar	105,0	104,5

5. Conclusions

The content of mercury in crude oil and natural gas is a present problem in oil & gas industry. The main concerns are related with its high toxicity and effect on the health & safety of the operators. However, there are only a few investigations on the matter. In fact, this is because mercury is present in crude oil and natural gas in trace levels, so Hg measurements are difficult to carry out. For this reason, thermodynamic models capable of simulating mercury behavior are needed.

In this Diploma thesis, an evaluation of mercury distribution in a typical natural gas processing plant was made by comparing two different models: SRK-Twu and UMR-PRU.

From the analysis of the results of the two models, it was concluded that both of them give reasonable results. The conclusions from the comparison of the models are the following:

- What concern the distribution of mercury, it was observed that the amount of mercury is higher in the liquid phase with SRK-Twu, with about 53% Hg recovery in the export condensate, while UMR-PRU predicts slightly higher mercury recovery in the vapor phase, with about 65% Hg recovery in the export gas.
- Furthermore, it was seen that both models predict a low solubility of mercury in water, as mentioned in literature.

The second step of this work was the sensitivity analysis in order to have a complete overview about the behavior of mercury in the plant when changing some natural properties and operating conditions. This analysis was divided into two parts, the first being the modification of the inlet feed, which involved the modification of the mercury content, the C_{7+} flowrates and the water content, while the second part concerned the modification of some operating conditions in the first three-phase separator (temperature and pressure). The sensitivity analysis gave similar results between the two thermodynamic models.

The conclusions from the sensitivity analysis can be summarized as follows:

- When molar composition of mercury in the inlet feed increases, the distribution of mercury in the different phases during separation and also the distribution

of all other components do not have any changes. Furthermore, it was observed that the specification of 10 ng/Sm^3 of Hg in the Export Gas is reached only when the molar composition of mercury in the inlet feed is 1 ppt and 1 ppb.

- When the C_{7+} flowrate increases, it was observed that, according to both models, more mercury partitions to the liquid phase. In addition, it was observed an increase of Pseudo components in the Export Condensate. In the Export Gas, an increase of Light components and a decrease of the Heavy and the Pseudo components was observed.
- By increasing the water content, the recovery of mercury in the vapor and liquid phases decrease slightly, while the recovery of mercury in the aqueous phase increases, for both models. Furthermore, it was observed that the distributions of all other components are almost the same for every water content examined.
- By decreasing the temperature in the first three-phase separator, the solubility of mercury in the liquid phase increases. Regarding the distributions of the other components, since vapor pressure decreases with decreasing temperature, in the Export Condensate, an increase of the Heavy components and a slight increase of the Light components are observed. As a consequence, in the Export Gas, a decrease of the Heavy and Pseudo components occurs, because they go in the liquid phase due to the decrease of the vapor pressure.
- When pressure decreases, an increase of vapor fraction occurs, which results in an increase of the amount of mercury in the vapor phase, a decrease in the liquid phase and a slight decrease also in the aqueous phase. Besides, for the distribution of the other natural gas components, it was observed that there is an increase of the Heavy components in the Export Gas. About Light components, first they increase and then they decrease. On the other hand, Pseudo components decrease. These trends, consequently, lead to a decrease of Light and Heavy components in the Export Condensate.

Finally, the value of cricondenbar for the Export Gas was also checked for each different pressure, and it was observed that the values were close between them.

In conclusion, the elemental mercury distribution of a typical natural gas processing plant was obtained. The lack of experimental data from the plant does not allow the clear evaluation of the two thermodynamic models. Nevertheless, the results from both of them are reasonable and comparable between them. Some sources in the literature, report Hg recovery in the export gas of the order of 80%, with the rest of the mercury being directed to the export condensate. So, in this case, only UMR-PRU gives similar results to the literature. Furthermore, even if mercury content in the streams is very low, deviations in mass balance are not too high.

6. Future work

The SRK-Twu and the UMR-PRU models were found to have some differences in the partitioning of mercury in the different phases during separation. However, possible actions to improve the mercury distribution models in natural gas could be the following:

- Acquisition of experimental data from the process in order to compare it with the results obtained and verify the models.
- Although elemental mercury is the main form found in natural gas, it is not the only form present. Furthermore, mercury could participate in some reactions with other compounds. So, chemical reactions and various Hg forms can be included in the models.
- Acquisition of solubility data for mercury in hydrocarbons and in other components that are of interest to the natural gas industry (e.g. helium), covering a large temperature range in order to better predict its distribution.
- Inclusion of the sweetening and dehydration processes and utilization of mercury solubility data in TEG, MEG, MEA, which are compounds used in these processes.

7. References

1. Wilhelm, S.M., *Mercury in Petroleum and Natural Gas: Estimation of Emissions from Production, Processing, and Combustion*. 2001, United States Environmental Protection Agency.
2. Panduan, G., *Guidelines on Mercury Management in Oil & Gas Industry*, M.o.H.R. Department of Occupational Safety and Health, Malaysia, Editor. 2011.
3. Ezzeldin, M.F., Z. Gajdosechova, M.B. Masod, T. Zaki, J. Feldmann, and E.M. Krupp, *Mercury Speciation and Distribution in an Egyptian Natural Gas Processing Plant.* Energy & Fuels, 2016. **30**(12): p. 10236-10243.
4. *Periodic Table* [cited 2018 15 March]; Available from: http://www.rsc.org/periodic-table.
5. Cotton, F.A. and G. Wilkinson, *Advanced Inorganic Chemistry*. 3rd ed. 1972: Interscience Publishers.
6. Boschee, P., *Advancements in the Removal of Mercury from Crude Oil.* Society of Petroleum Engineers, 2013 **2**(2).
7. Mentzelos, C., *Modelling of mercury (Hg) distribution in a natural gas processing plant*. 2014, Norwegian University of Science and Technology.
8. Gallup, D.L., D.J. O'Rear, and R. Radford, *The behavior of mercury in water, alcohols, monoethylene glycol and triethylene glycol.* Fuel, 2017. **196**: p. 178-184.
9. *Phase and Chemical Equilibrium Modelling of Natural Gas Mixtures Containing Hg - Report*. 2018, National Technical University of Athens - Thermodynamics & Transport Phenomena Laboratory
10. Marsh, K.N., J.W. Bevan, J.C. Holste, D.L. McFarlane, M. Eliades, and W.J. Rogers, *Solubility of Mercury in Liquid Hydrocarbons and Hydrocarbon Mixtures.* Journal of Chemical & Engineering Data, 2016. **61**(8): p. 2805-2817.
11. Lide, D.R. and H.V. Kehiaian, *CRC handbook of thermophysical and thermochemical data*. Vol. 1. 1994: Crc Press.
12. Snell, J.P., W. Frech, and Y. Thomassen, *Performance improvements in the determination of mercury species in natural gas condensate using an on-line amalgamation trap or solid-phase micro-extraction with capillary gas chromatography-microwave-induced plasma atomic emission spectrometry.* Analyst, 1996. **121**(8): p. 1055-1060.

13. Daubert, T.E. and R.P. Danner, *Physical and thermodynamic properties of pure chemicals : data compilation*. 1994, New York: Hemisphere Pub. Corp.
14. Twu, C.H., J.E. Coon, and J.R. Cunningham, *A new generalized alpha function for a cubic equation of state Part 2. Redlich-Kwong equation.* Fluid Phase Equilibria, 1995. **105**(1): p. 61-69.
15. Chorng H. Twu, D.B., John R. Cunningham, John E. Coon, *A cubic equation of state with a new alpha function and a new mixing rule* Fluid Phase Equilibria, 1991. **69**: p. 33-50.
16. T.Y. Kwak, G.A.M., *Van der Waals mixing rules for cubic equations of state, applications for supercritical fluid extraction modelling* Chemical Engineering Science, 1986. **41**: p. 1303-1309.
17. Koulocheris, V., V. Louli, E. Panteli, S. Skouras, and E. Voutsas, *Thermodynamic modelling of elemental mercury solubility in natural gas components.* Fuel 2018.
18. Voutsas, E., K. Magoulas, and D. Tassios, *Universal Mixing Rule for Cubic Equations of State Applicable to Symmetric and Asymmetric Systems: Results with the Peng−Robinson Equation of State.* Industrial & Engineering Chemistry Research, 2004. **43**(19): p. 6238-6246.
19. Peng, D.-Y. and D.B. Robinson, *A New Two-Constant Equation of State.* Industrial & Engineering Chemistry Fundamentals, 1976. **15**(1): p. 59-64.
20. Mathias, P.M. and T.W. Copeman, *Extension of the Peng-Robinson equation of state to complex mixtures: Evaluation of the various forms of the local composition concept.* Fluid Phase Equilibria, 1983. **13**: p. 91-108.
21. Skouras, D.S., *Natural Gas Processing - Presentation*. 2017, Statoil.
22. Mokhatab, S., W.A. Poe, and J.G. Speight, *Handbook of Natural Gas Transmission and Processing* 2006: Gulf Professional Publishing.